



HAL
open science

Forecasting contrasting coastal and estuarine hydrodynamics with OPENCoastS

Anabela Oliveira, André B Fortunato, Marta Rodrigues, Alberto Azevedo, João Rogeiro, Samuel Bernardo, Laura Lavaud, X. Bertin, Alphonse Nahon, Gonçalo de Jesus, et al.

► **To cite this version:**

Anabela Oliveira, André B Fortunato, Marta Rodrigues, Alberto Azevedo, João Rogeiro, et al.. Forecasting contrasting coastal and estuarine hydrodynamics with OPENCoastS. *Environmental Modelling and Software*, 2021, 143, pp.105132. 10.1016/j.envsoft.2021.105132 . hal-03454644

HAL Id: hal-03454644

<https://univ-rochelle.hal.science/hal-03454644v1>

Submitted on 29 Nov 2021

HAL is a multi-disciplinary open access archive for the deposit and dissemination of scientific research documents, whether they are published or not. The documents may come from teaching and research institutions in France or abroad, or from public or private research centers.

L'archive ouverte pluridisciplinaire **HAL**, est destinée au dépôt et à la diffusion de documents scientifiques de niveau recherche, publiés ou non, émanant des établissements d'enseignement et de recherche français ou étrangers, des laboratoires publics ou privés.

Forecasting contrasting coastal and estuarine hydrodynamics with OPENCoastS

A. Oliveira,^{1,*} A.B. Fortunato,¹ M. Rodrigues,¹ A. Azevedo,¹ J. Rogeiro,¹ S. Bernardo,² Laura Lavaud,³ Xavier Bertin,³ Alphonse Nahon,¹ Gonçalo de Jesus,¹ Miguel Rocha,¹ P. Lopes¹

1 - National Laboratory for Civil Engineering, Av. do Brasil, 101, 1700-066 Lisbon, Portugal

2- LIP, Av. Gama Pinto, n.2, piso 3. Complexo Interdisciplinar (3is) 1649-003 Lisboa

3 - UMR 7266 LIENSs, CNRS-La Rochelle Université, 2 rue Olympe de Gouges, 17000 La Rochelle, France.

*** Corresponding author**

Submitted to Environmental Modeling & Software, April, 2021

Reviewed, July, 2021

Highlights

- Web platform to generate on-demand forecast systems for multiple circulation options
- Open source software at <https://opencoasts.ncg.ingrid.pt/>, using EOSC resources
- Forced by GFS, WRF or ARPEGE (atmosphere), CMEMS or FES2014 (ocean) and WW3 (waves)
- Data/model comparison with Copernicus Sentinel data and in-situ EMODnet field data

Abstract

1 Robust and accurate coastal forecasts require models to represent the relevant
2 processes, prediction computational tools and reliable computational resources.
3 OPENCoastS is a free, open-source WebGIS platform to develop on-demand
4 hydrodynamic forecast systems that started as a simple 2D engine.
5 OPENCoastS provides a visualization and download interface with in-situ and
6 Sentinel satellite data comparison. 2D tidal, 2D wave & current interaction and
7 3D baroclinic flows are now included, forced by several atmospheric, oceanic
8 and riverine forcings.
9

10 Four applications demonstrate OPENCoastS' capacity. The prediction of the
11 2020 typhoon season in Taiwan illustrates the use of the service using only
12 large-scale public data. An application to the Bay of Biscay shows the
13 importance of waves on extreme water levels during storms. A nearshore
14 deployment in Figueira da Foz harbor assesses the impact of bathymetry on
15 coupled wave and current circulation. 3D baroclinic circulation forecasts in
16 Tagus estuary are validated by independent data.
17

18 **Keywords:** SCHISM, Forecast systems, Unstructured grids, cross-scale, EOSC,
19 Wave and currents modeling, Baroclinic modeling
20

21 **Software availability**

22 Program title

23 OPENCoastS

24 Developers

25 João Rogeiro, Joana Teixeira, Pedro Lopes, Gonçalo de Jesus, Miguel
26 Rocha, Alberto Azevedo, Marta Rodrigues, André Fortunato
27

28 Contact address

29 jrogeiro@lnec.pt

30 Software Access

31 <https://opencoasts.ncg.ingrid.pt/>

32 Year first available

33 2018 (v1); 2021 (v2)

34 Software required

35 Browser: Firefox, Google Chrome
36
37
38
39
40
41
42
43
44
45
46
47
48
49
50
51
52
53
54
55
56
57
58
59
60
61
62
63
64
65

1 Program language
2 Python & HTML+CSS+JavaScript
3

4 Availability and cost

5 Access for usage: Open access upon registration (email required)
6

7
8 Access to source code: Free software with an Apache License Version 2.0
9 available in: <https://gitlab.com/opencoasts/eosc-hub>
10
11

12 13 14 **1. Introduction** 15

16
17 Coastal forecast systems provide predictions of environmental variables at time
18 scales of a few days. Environmental variables include water levels, velocities,
19 wave parameters, pollutant concentrations and sediment fluxes. These forecast
20 systems have a wide range of applications in coastal and harbor management
21 (Viegas et al., 2009; Bedri et al., 2014; Oliveira et al., 2015), civil protection
22 (Breivik and Allen, 2008; Fortunato et al., 2017a; Ferrarin et al., 2019; Stokes et
23 al., 2020), navigation (Orseau et al., 2021), military operations and recreation
24 (e.g. windguru.cz, magicseaweed.com). Some of these forecast systems cover
25 spatial scales from oceans and regional seas to coastal regions, using
26 downscaling techniques over structured and unstructured grids (Trotta et al.,
27 2016, 2021). They are developed and operated by research centers,
28 meteorological and hydrographic organizations, harbor administrations and
29 private companies.
30

31
32 In spite of the growing development of coastal forecast systems, their
33 dissemination remains limited by their implementation and maintenance costs.
34 These costs are mostly associated with very specialized human resources, with
35 backgrounds in both numerical modeling and information technologies, and also
36 with dedicated computational resources to guarantee a timely delivery of
37 predictions.
38

39
40 However, several evolutions are paving the way for a drastic increase in the
41 development and adoption of coastal forecast systems. First, higher resolutions,
42 more stable numerical schemes and better parameterizations reduce the need for
43 calibration and the effort required to optimize the numerical parameters. As a
44 result, the skills required from modelers decrease and forecasts become more
45 robust. Second, the growing availability of online near-real time data (e.g.,
46 GEMCO, EMODNET), atmospheric forecasts (e.g., GFS, WRF, ARPEGE) and
47 large-scale ocean models (e.g., FES2014, CMEMS, HYCOM) provide free
48
49
50
51
52
53
54
55
56
57
58
59
60
61
62
63
64
65

1 access to the information required to force local forecasts worldwide. Third,
2 large computational infrastructures, both public and commercial, can now
3 provide the computational power to perform demanding simulations without the
4 need to acquire and operate these infrastructures. The European Open Science
5 Cloud (EOSC) and the Partnership for Advanced Computing in Europe
6 (PRACE) are examples of such public infrastructures.
7

8
9 A fourth evolution that can drastically reduce the cost of generating and
10 operating coastal forecast systems is automation. The recent development of
11 Web-based platforms that can simultaneously generate and operate coastal
12 modeling systems with minimal human intervention will reduce the cost of
13 forecast systems, thereby fostering their dissemination. Examples of these tools
14 remain scarce in the coastal and ocean communities. WebMARVL (the Virtual
15 Marine Laboratory, Oke et al., 2016), for setting up ocean circulation and wave
16 models, Delft-FEWS, dedicated to hydrological and coastal flood forecasting
17 (Werner et al., 2013), and OPENCoastS, to generate coastal forecast systems for
18 any location in a few minutes (Oliveira et al. 2020) are the most comprehensive
19 platforms available. OPENCoastS is a user-friendly platform supported by
20 EOSC computational services and resources. It is freely available to all users
21 whereas, for instance, WebMARVL is dedicated to the Australian communities.
22 The original version of the platform described in Oliveira et al. (2020) was
23 however limited to simple physics (i.e., 2D depth-averaged shallow water
24 flows). Now it has matured and addresses more complex flows, including wave
25 and currents interactions and 3D baroclinic flows. The only inputs requested to
26 the users to set up a new deployment are the horizontal grid file and, for the 3D
27 runs, also the vertical grid. The platform is maintained in operation through the
28 use of European Open Science cloud (EOSC) resources and forecasts still take
29 only a few minutes to generate.
30

31 This paper aims at demonstrating how forecast systems built using the
32 OPENCoastS service can provide accurate prediction of complex flows in
33 estuarine and coastal environments. “Complex flows” refer here to flows
34 associated with extreme atmospheric events, breaking waves, and strong density
35 gradients, and at scales ranging from tens of meters to thousands of kilometers.
36 Four demonstration examples are presented herein that cover various spatial
37 scales (from basin-wide to estuarine scales), different forcing agents (tides,
38 waves, river flow, wind and atmospheric pressure), applied in distinct
39 geographies (European and Asian coasts). These examples address different
40 scientific questions (e.g., coastal inundation, salinity dynamics in estuaries) and
41
42
43
44
45
46
47
48
49
50
51
52
53
54
55
56
57
58
59
60
61
62
63
64
65

the forcing agents include tides, waves, river flow, wind and atmospheric pressure. The criteria behind the selection of the applications are summarized in Table 1. The evolution of the platform, from its original version to its present capabilities, is also detailed to promote the usage of the service software by other teams. It is now freely available under licence Apache License Version 2.0 at <https://gitlab.com/opencoasts/eosc-hub/webportal>.

The paper is organized as follows. First, the OPENCoastS platform is briefly described, with an emphasis on the most recent features. Then, the capabilities of the platform to support operational management in coastal systems are demonstrated through four examples of application. In section 3, these examples are used to illustrate and discuss the lessons learned from the first three years of development of OPENCoastS. Finally, the potential and the present limitations of OPENCoastS are discussed and its evolution is anticipated.

Table 1 - Characterization of the demonstration cases

	Coast of Taiwan	Bay of Biscay	Figueira da Foz Harbor	Tagus Estuary
basin scale	X	X		
coastal/estuarine scale			X	X
2D barotropic	X	X	X	
3D baroclinic				X
waves		X	X	
no waves	X			X

2. OPENCoastS service version 2: general description

2.1 Overview of the OPENCoastS service

The OPENCoastS service provides accurate circulation forecasts in any coastal system of choice (Oliveira et al., 2020). This is achieved through the use of the process-comprehensive suite of numerical models provided by SCHISM (Zhang et al., 2016), and of a complex computational web platform. SCHISM was chosen because it encompasses all relevant processes, and the web platform was built to run it seamlessly and automates the whole prediction workflow. This combination provides the users the capacity to efficiently build, manage and visualize forecasts. Initially developed as a simple 2D forecast engine (Oliveira et al., 2020), OPENCoastS is now a full-fledged service that simulates all types of estuarine and coastal circulation options: 2D barotropic, 2D waves and currents interaction and 3D baroclinic circulation. Herein, we start by summarizing the architecture and main characteristics of the service and its implementation in the EOSC infrastructure. The implementation of the new circulation functionalities and their dependencies for input file building is detailed afterwards, along with the new options for both ocean forcings and data comparison.

The OPENCoastS service aims at addressing the following properties: Broad availability, Simplicity and user-friendliness, Comprehensiveness, Accuracy and reliability, Flexibility and Modularity (Oliveira et al., 2020). These properties are achieved in the current full circulation service, to guarantee the quality of the final forecasts. Moreover, the architecture to address the properties of modularity and flexibility is paramount to continue to accommodate any new functionalities in the future while maintaining a coherent, simple and user-friendly platform. The service is available at <https://opencoasts.ncg.ingrid.pt> and is organized along the “Configuration assistant”, which guides the assemblage of the site-specific forecast systems; the “Forecast systems manager”, through which users monitor and act upon their forecasts; and the “Outputs viewer” where users visualize and download model’s input and output files (Figure 1). The complete workflow of the Configuration assistant in the OPENCoastS web app is summarized in Figure 2, highlighting the detailed approach to account for the several circulation options requirements.

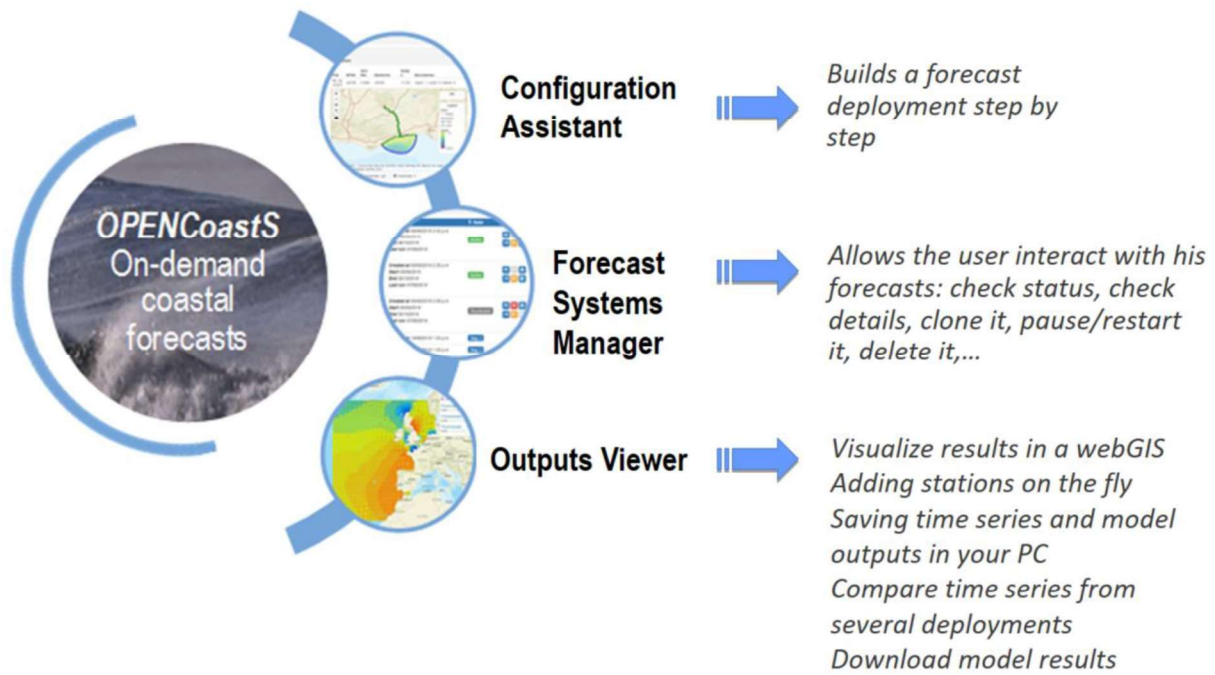


Figure 1: OPENCoastS frontend components

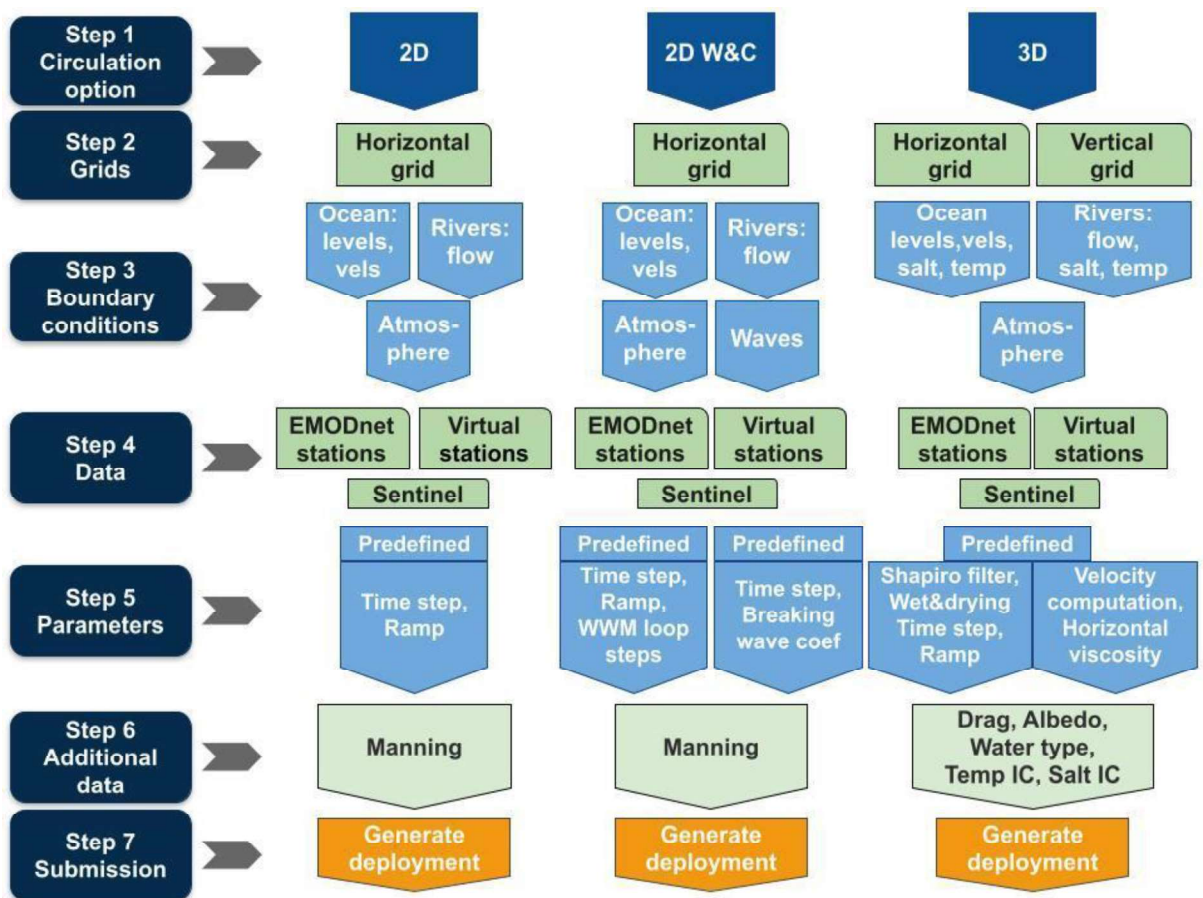


Figure 2. Workflow of the Configuration assistant for the several circulation options.

2.2 Current application of SCHISM modeling suite in OPENCoastS

The OPENCoastS evolution to complete coastal physics was made possible by the comprehensive representation of physical processes available in the SCHISM modeling suite (Zhang et al., 2016; <http://ccrm.vims.edu/schismweb>), the open-source modeling engine behind OPENCoastS. SCHISM is an open-source community-supported modeling system designed for a seamless cross-scale simulation from creek to ocean and is used here in version v5.4.1. The model is fully parallelized, to optimize the computing times in forecast applications.

SCHISM has been extensively tested against ocean/coastal benchmarks (Chen et al., 2013; Lynett et al., 2017) and applied to several regional seas, embayments and estuaries worldwide in the fields of general circulation, tsunami, storm-surge and compound inundation, wave-current interaction, water quality, coastal ecology, and morphodynamics (e.g., Guérin et al., 2016; Rodrigues and Fortunato, 2017; Fortunato et al., 2017b; Allen et al., 2018; Li et al., 2018; Du et al., 2020; Wang et al., 2020; Lavaud et al., 2020; Huang et al., 2021). SCHISM is also the hydrodynamic engine of several forecast systems besides OPENCoastS (Stanev et al., 2016; Fortunato et al., 2017a; Chiu et al., 2018; Fernandez-Montblanc et al., 2019).

SCHISM solves the three-dimensional shallow water equations and computes the free-surface elevation and the 3D water velocity, salinity and temperature fields using finite-element and finite-volume schemes. The simultaneous solution of continuity and momentum equations, and a highly efficient semi-implicit finite-element Eulerian-Lagrangian algorithm bypass the most severe stability restrictions (e.g. associated with the Courant number). Mass conservation can be enforced by upwind or finite-volume transport algorithm (TVD2) methods. The natural incorporation of wetting and drying makes the model suitable for inundation studies. In OPENCoastS, the wave model WWM (Roland et al., 2012) is fully coupled in 2DH with SCHISM, and the two models share the same computational grid and domain decomposition. When this option is activated, WWM provides the circulation model with wave forces computed according to the radiation stress formalism of Longuet-Higgins and Stewart (1964) and the circulation model provides WWM with fields of water levels and depth-averaged velocities. SCHISM discretizes the domain using unstructured grids in the horizontal, which allows a greater flexibility in

1
2
3
4
5
6
7
8
9
10
11
12
13
14
15
16
17
18
19
20
21
22
23
24
25
26
27
28
29
30
31
32
33
34
35
36
37
38
39
40
41
42
43
44
45
46
47
48
49
50
51
52
53
54
55
56
57
58
59
60
61
62
63
64
65

representing the bathymetry, and hybrid SZ coordinates or LSC² (Zhang et al., 2015) along the vertical.

In OPENCoastS, only horizontal grids with triangular elements and vertical grids based on hybrid SZ coordinates can be used, in spite of other discretization options available in SCHISM. Forcing conditions at the ocean boundaries in OPENCoastS include both elevation and velocities if FES2014 is used, providing more accurate results, or just elevations, for the other forcing options. For 3D simulations, forcing conditions at the oceanic boundaries also include space and time varying salinity and temperature. At the river boundaries, forcing conditions can be set up as constant or as time varying. Those include river flows for 2D simulations and river flows, salinity and temperature for 3D simulations. OPENCoastS is organized along three circulation options, depending on the relevant physics. A summary of the inputs and outputs is presented below along with the new features.

1) 2D barotropic simulations

These simulations output water levels and depth-averaged velocities. The circulation is forced by tides, wind, atmospheric pressure and river flow. This option corresponds to the first version of OPENCoastS, with a minor improvement of forcing both elevation and velocities at the ocean boundaries. The reader is referred to Oliveira et al. (2020) for further details.

2) 2D barotropic simulations with wave-current interaction (2D W&C)

In addition to Option 1, these simulations also provide wave parameters. All wave-current interactions are simulated, including the effect of water levels and depth-averaged currents on wave propagation and the wave forces on the mean flow through the wave radiation stress gradients. Inside the domain, WWM is forced by the same surface winds as the circulation model. WWM is also forced along its open boundaries by time series of directional spectra computed from an application of the WaveWatch III model (WW3, version 5.16) (The WAVEWATCH III R Development Group, 2016) to the North Atlantic (grid is shown in Supplementary material #1). As spectra for larger domains are not freely available online, this option can only be used for domains forced by North Atlantic waves. Each deployment has its own WW3 runs, to generate the necessary boundary conditions. A master WW3 is also maintained to provide hot-start conditions for each new deployment's forcing WW3 run (Figure 3), avoiding cold-start conditions or the need to start the forecast deployment

several days in the past. The wave and current backend workflow is highlighted in Figure 3.

current backend workflow is

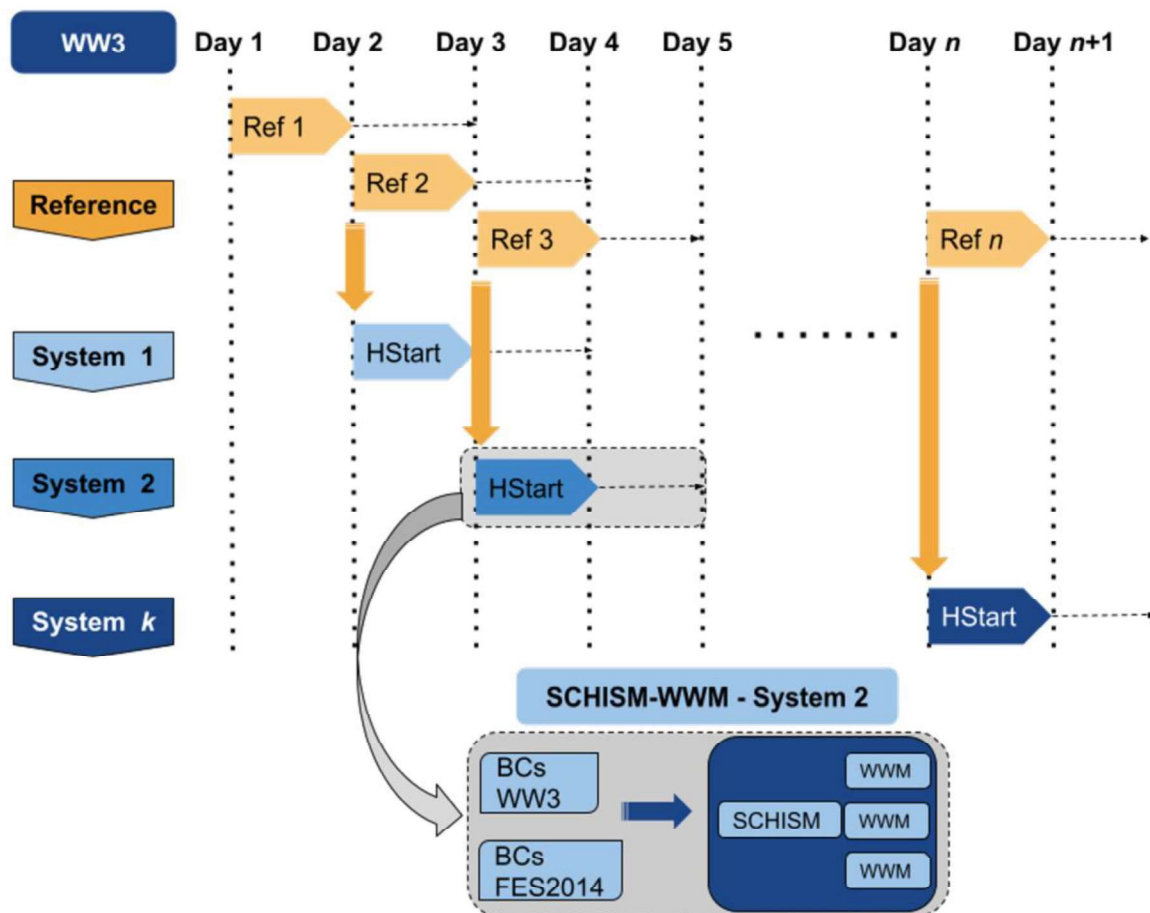


Figure 3: Backend workflow for waves & currents option: procedure for hot starting the waves' simulation. The inset illustrates the procedure for each simulation, with the possibility of having multiple WWM runs for one time step of SCHISM or the opposite situation.

3) 3D baroclinic simulations - these simulations provide 3D fields of velocity, salinity and water temperature, besides water levels. They can be forced by tides, river flow, temperature and salinity at all the boundaries, and also by the atmospheric surface forcing (wind, air temperature, pressure, humidity, solar radiation and downwelling longwave radiation).

Boundary conditions for 3D velocities, salinity and temperature at the ocean boundaries are provided by CMEMS (<https://marine.copernicus.eu/>), with two sources available: CMEMS Global and Iberian-Biscay-Ireland (IBI) regional seas. These sources can also be used to force water elevations in other

1 circulation options as part of the ocean boundary conditions portfolio.
2 Atmospheric inputs for these runs can be obtained with GFS or WRF, both
3 provided by NOAA. At the rivers' boundaries, besides annual and monthly
4 values, a web provider for time series can also be used to provide flow forecasts
5 every day. Finally, one river flow can also be specified as a percentage of
6 another one, either defined as monthly or annual values or through an external
7 river forecast provider.
8
9

10
11
12 Unlike the wave and current interaction option, 3D baroclinic forecasts can
13 be generated anywhere in the world. The forcing of the salinity and temperature
14 ocean boundaries can only be done with one of the two CMEMS options:
15 Global or IBI.
16
17
18

19
20 The Forecast systems manager provides multiple actions on forecasts 1)
21 conclude deployment; 2) pause and cancel a deployment and 3) cloning a
22 deployment, besides monitoring the status of the runs and providing alerts for
23 the near conclusion of the operating period. The cloning facility is used
24 frequently as it provides a very efficient way to perform sensitivity analyses on
25 parameters and forcings for a specific site.
26
27
28
29

30
31 The Outputs viewer presents results from all circulation options. Besides the
32 inclusion of the new variables depending on the type of deployment selected,
33 the capacity to see 3D results along the vertical (and to compare different levels)
34 was also added. Downloading facilities were extended for the new files
35 generated in the additional options.
36
37
38
39

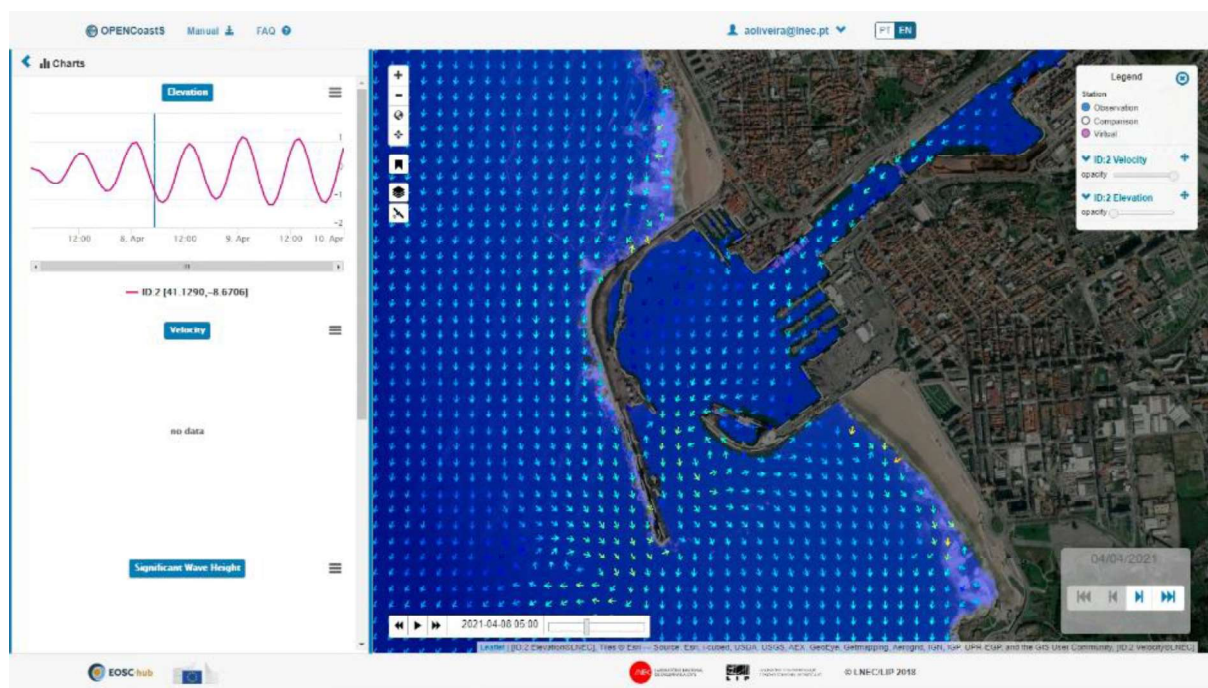
40 41 2.3 Data comparison options in OPENCoastS 42

43 Automatic comparison with field data validates the quality of the predictions
44 and supports the usefulness of the tool and the users' confidence in its results.
45 OPENCoastS is linked to the EMODNET Physics elevation data hub
46 (<https://portal.emodnet-physics.eu/>). The user selects the stations for the
47 model/data comparison for each deployment in the Configuration assistant and
48 then visualizes the data against the results in the viewer.
49
50
51
52

53
54 Comparison with remote sensing data is also available, to determine the
55 interface between land and water (extent of inundation), based on images from
56 the Sentinel satellites. The possibility of comparing model results with a
57 processed Sentinel image is integrated in the Configuration assistant. If the user
58
59
60
61
62
63
64
65

1 selects the comparison with remote sensing option, the OPENCoastS workflow
2 starts a regular procedure to download images from the ESA Copernicus
3 OpenHub, crops them to the limits of the deployment horizontal grid, binarizes
4 it to determine the land-water interface and converts it to a raster. The rasters
5 are stored in a database and are connected to the respective deployment ID.
6 Upon entering the viewer page, the OPENCoastS interface builds a JSON file
7 with the latest rasters.
8
9

10
11
12 In the viewer, the users can select the visualization of the Sentinel-based layers
13 against the model results. As Sentinel images have a specific time stamp, we
14 provide the capacity to overlap each simulation with the nearest processed
15 image. This visual comparison is available for the whole simulation, regardless
16 of the specific time step that would be closest to the Sentinel time stamp. The
17 rasters are loaded into the map with an opacity applied to them to facilitate the
18 comparison with the model forecasts (Figure 4).
19
20
21
22
23
24



25
26
27
28
29
30
31
32
33
34
35
36
37
38
39
40
41
42
43
44
45
46
47
48
49 Figure 4 - Comparison between the water limit extracted from Sentinel 2 images
50 (in blue) and the OPENCoastS prediction (velocity field). The brown dashed
51 line marks the limit of the grid, which represents the Leixões harbor and
52 Matosinhos Beach in Northern Portugal.
53
54

55
56
57 New satellite images are downloaded and added to the system at the beginning
58 of each day. Upon selecting the option to download the images, as there will not
59
60
61
62
63
64
65

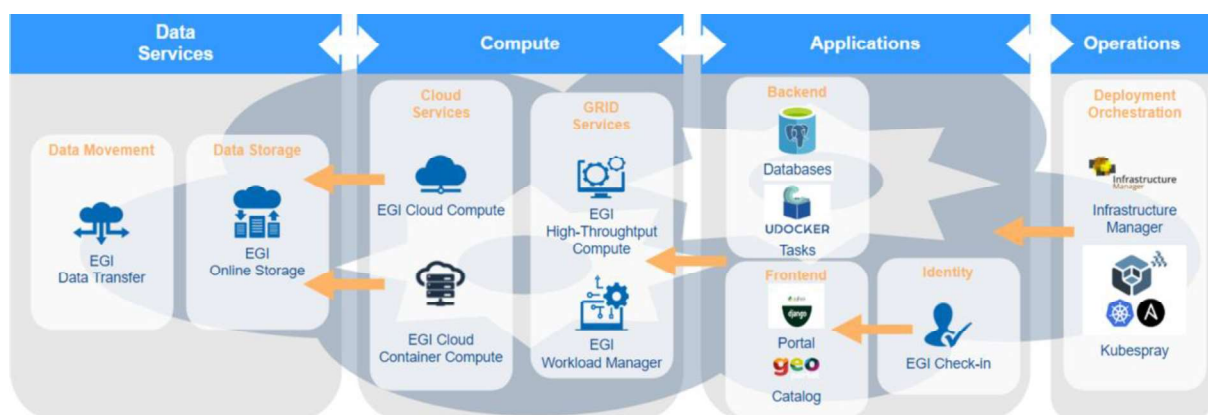
1 be any images available on the database, OPENCoastS checks back in time to
2 retrieve the images available from the last five days.
3
4

5 2.4 Brief description of the implementation of OPENCoastS in the 6 EOSC infrastructure 7

8
9 During the last decade, Global Open Science emerged as a trusted digital
10 platform to support the scientific community. The European project EOSC-hub
11 aimed to foster the best practices for data and services management, simplifying
12 the researchers' access to available infrastructure sites. OPENCoastS is one of
13 the seven thematic services integrated in the EOSC infrastructure in the scope of
14 this project (<https://marketplace.eosc-portal.eu/services/opencoasts-portal>).
15
16

17 The OPENCoastS service requires high availability of computational resources
18 to guarantee the delivery of forecast outputs in due time. Portugal's National
19 Distributed Computing Infrastructure (INCD) and Cantabria Physics Institution
20 (IFCA) offer the required facilities for OPENCoastS simulations, providing the
21 integration with the core EOSC-hub services for authentication, accounting,
22 computation and data preservation.
23
24

25 OPENCoastS comprehends several components, such as catalogs of model
26 data/results and their metadata, SCHISM processing scripts, a web
27 Configuration assistant, a web portal for managing the user accounts and
28 applications, and a web map visualization tool. These components were
29 integrated with the EOSC core services summarized in Figure 5. Available core
30 services were promoted within EOSC-hub to support OPENCoastS and other
31 thematic services (<https://marketplace.eosc-portal.eu/services/c/access-physical-infrastructures>).
32
33
34
35
36
37
38
39
40
41
42



57 Figure 5. OPENCoastS integration with EOSC services
58
59
60
61
62
63
64
65

1 The main supporters of those core services are the European Grid Initiative
2 (EGI), for cloud and grid services, and EUDAT for storage. Authentication
3 Authorization and Identity (AAI) is available in both EUDAT and EGI
4 portfolios, which implement the AARC Blueprint Architecture ([https://aarc-
5 project.eu/architecture/](https://aarc-project.eu/architecture/)), supporting communities users' with subordinate end
6 services.
7

8
9 The current implementation of OPENCoastS in the INCD infrastructure uses the
10 following core services: EGI Cloud Compute, EGI Online Storage and EGI
11 Check-in for AAI. These EOSC core services enable the deployment of the
12 OPENCoastS applications and provide the endpoint for the portal. Additionally,
13 SCHISM's processing work and all related tasks are submitted to EGI
14 Workload Manager. This manager distributes the computational demand by all
15 available resource sites using EGI High-Throughput Compute. The software
16 requirements and dependencies are encapsulated in a docker image that is
17 loaded in the computing nodes with the udocker tool (Gomes et al., 2018).
18 Udocker allows pulling and executing docker containers in Linux batch systems
19 and interactive clusters in user space without requiring root privileges. A bundle
20 that encapsulates the whole OPENCoastS service and its installation at a user-
21 defined infrastructure is freely distributed at the GitLab repository in
22 <https://gitlab.com/opencoasts/eosc-hub/webportal>.
23
24
25
26
27
28
29
30
31
32
33

35 **3. OPENCoastS applications**

36 3.1. Extreme water levels in the coast of Taiwan

37
38 The northwestern Pacific Ocean is the most active tropical cyclone basin on
39 Earth (Elsner and Liu, 2003). The most severe of these cyclones, locally known
40 as typhoons, can generate extreme storm surges that can have devastating
41 effects on the shores of the Philippines, China, Taiwan and Japan. Here, we
42 illustrate the generation of a forecast system for the coast of Taiwan with
43 OPENCoastS and its validation using only publicly available data.
44
45
46
47
48

49 Typhoon tracks can be divided into three groups (Elsner and Liu, 2003). Taiwan
50 is affected by typhoons following two of these groups: the straight track, a
51 general westward path, and the parabolic recurving track, which follows to the
52 North-west and then turns north. The model domain (Figure 6) was thus defined
53 such that it contains these typhoon tracks. The coastal boundary was defined
54 using the Global Self-consistent, Hierarchical, High-resolution Shoreline
55 database (https://gnome.orr.noaa.gov/goods/tools/GSHHS/coast_subset), and
56
57
58
59
60
61
62
63
64
65

1
2
3
4
5
6
7
8
9
10
11
12
13
14
15
16
17
18
19
20
21
22
23
24
25
26
27
28
29
30
31
32
33
34
35
36
37
38
39
40
41
42
43
44
45
46
47
48
49
50
51
52
53
54
55
56
57
58
59
60
61
62
63
64
65

the bathymetry was extracted from the General Bathymetric Chart of the Oceans (<https://download.gebco.net>). A grid with 93,000 nodes was generated by automatically placing the nodes with a specified spatially-varying resolution using the program xmgredit (Turner and Baptista, 1993). This resolution varies between 1-2 km around Taiwan and 10-16 km in the deep ocean. Then, this preliminary grid was automatically improved using the program nicegrid (Fortunato et al., 2011). The resulting number of elements linked to each node varies between 5 and 7 to ensure a smooth transition between element sizes. Because the domain is very deep, friction is expected to be negligible. The Manning coefficient was set to $0.022 \text{ m}^{1/3}/\text{s}$ throughout the domain, and the model was not calibrated. The time step was specified as 240 s, as proposed by OPENCoastS.

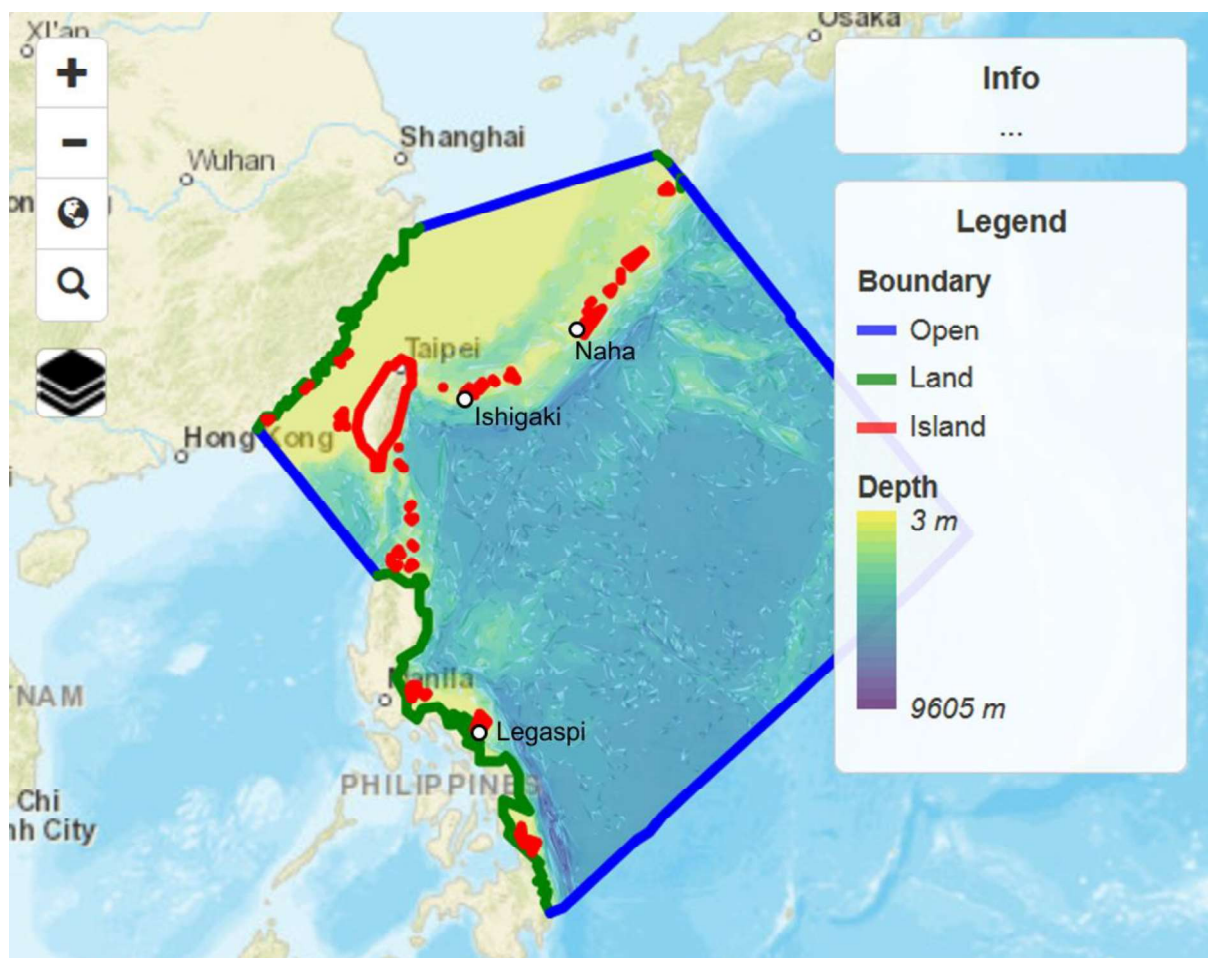


Figure 6. Taiwan typhoon model domain, bathymetry and tide gauges (circles)

SCHISM was forced at the sea surface by winds and atmospheric pressure from GFS, and at the open boundaries by tides from FES2014 (Lyard et al., 2020) and the inverse barometer effect.

Forecasts were produced in OPENCoastS for the 2020 typhoon season (July to September). During this period, 14 tropical storms occurred in the Pacific, including typhoons Hagupit (July 31 – August 5), Bavi (August 21 – August 27), Maysak (August 27 – September 3) and Haishen (August 31 – September 9). Haisen, in particular, peaked as a Category 4 typhoon. The model was validated using sea surface height data from the three stations located within the domain (Figure 6) and available at the EMODnet platform. The data time series include numerous gaps.

Table 2. Validation of the Taiwan forecasts: unbiased root mean square errors (URMSE) and normalized unbiased root mean square errors (NURMSE). NURMSE are normalized by the standard deviation of the data.

Station	Ishigaka	Legaspi	Naha
URMS (m)	0.10	0.05	0.07
NURMS (%)	25	12	14

Comparison with field data shows that the model reproduces sea surface heights with unbiased root mean square errors between 5 and 10 cm (Table 2). These errors correspond to 12 to 25% of the standard deviation of the measured sea surface height. The RMSE obtained with OPENCoastS compare favorably with a recent application to the same area (Liu and Huang, 2020).

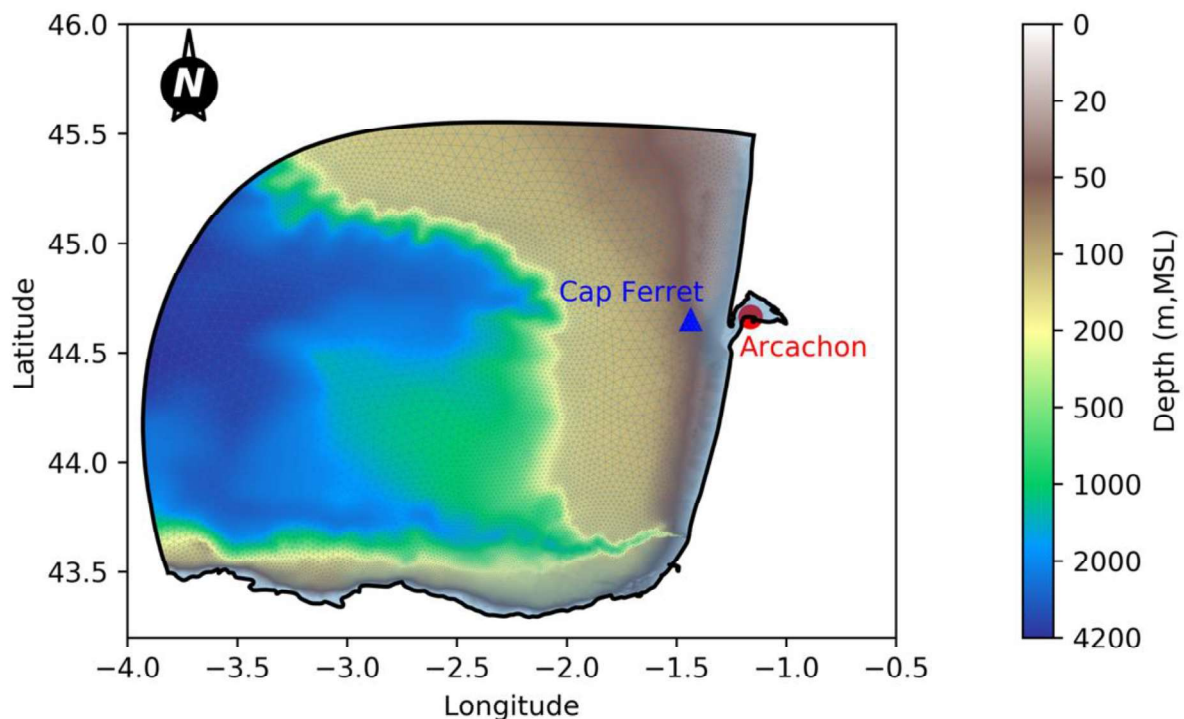
The model accuracy could certainly be improved. A comparison between the shoreline database and satellite images shows that the data are coarse and outdated in some areas. Calibration of the friction coefficient in the continental shelf between Taiwan and China, which would require tide gauge data in that area, would probably improve the water levels prediction locally. More importantly, including waves would increase the storm surge. The importance of waves on storm surges was shown by Chen et al. (2017) for this particular region, and is also shown in the next section for the Bay of Biscay.

In spite of these limitations, this application shows that adequate forecasts can be quickly obtained with OPENCoastS without any a priori knowledge of the

1 study region and using only open data and model results for the model setup and
2 validation.
3
4

5 3.2. Storm waves and surge in the Bay of Biscay 6

7 The Bay of Biscay is exposed to severe winter storms, which can drive waves of
8 significant height (hereafter H_s) over 10 m, storm surges over 1.5 m (Bertin et
9 al., 2015; Lavaud et al., 2020) and catastrophic marine flooding (Bertin et al.,
10 2014). The storm Justine hit the central part of the Bay of Biscay on 31st of
11 January 2021 and drove waves of H_s reaching 10 m in the deep ocean and over
12 8 m at the nearshore buoy Cap Ferret (Figure 7). Inside the Arcachon Lagoon
13 (Figure 8), water level measurements suggest that a storm surge of about 1.0 m
14 developed. In this section, we present a fully-coupled 2DH high resolution
15 forecast of the sea state and water levels associated with this storm to
16 demonstrate the relevance of short waves in OPENCoastS.
17
18
19
20
21
22
23
24



49 Figure 7. Bathymetric map and extension of the computational domain
50 with location of the Arcachon tide gauge (red circle) and the Cap Ferret buoy
51 (blue triangle).
52

53 The unstructured grid used to perform the forecast covers the southern part of
54 the Bay of Biscay (Figure 7) and comprises 60060 nodes and 117303 triangular
55 elements, with a spatial resolution ranging from 5500 m along the open
56 boundary to 80 m at the entrance of the Arcachon Lagoon. Along the open
57
58
59
60
61
62
63
64
65

boundary, the circulation model was forced by amplitudes and phases of the 34 main tidal constituents from FES2014 (Lyard et al., 2020). Over the whole domain, the circulation model was forced by 10 m wind speed and sea-level pressure issued from ARPEGE atmospheric forecasts and an inverse barometer condition was applied along the open boundary. ARPEGE wind fields were also used to force the wave model WWM. Along the open boundary, WWM was forced by time-series of directional wave spectra, which were computed from WW3 forced with wind fields from the GFS atmospheric model. The time steps were set to 30 s and 300 s in the hydrodynamic and wave model, respectively.

The model predictions were first compared against observed significant wave height (H_s), mean absolute wave period (T_{m02}) and mean wave direction (Mwd) available at the Cap Ferret Buoy, located 14 km from the coast by a mean water depth of 50 m. This comparison reveals that H_s and T_{m02} are very well reproduced, with normalized root mean square errors (NRMSE) of 12 and 8 %, respectively. Mwd is also well reproduced, with a root mean square error (RMSE) lower than 5° (Figure 8).

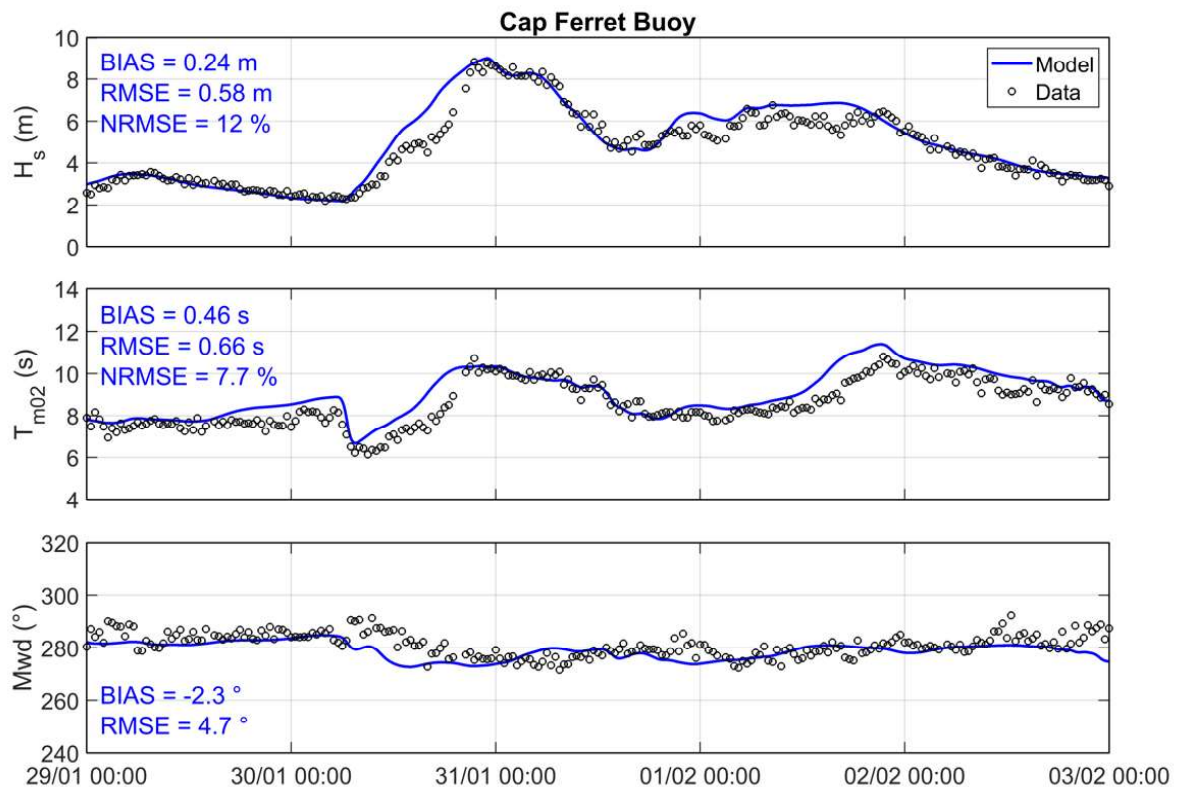


Figure 8. Modeled (blue) against observed (black circles) significant wave height (H_s), mean absolute wave period (T_{m02}) and mean wave direction (Mwd) at Cap Ferret Buoy during storm Justine. Normalized root mean square errors (NRMSE) are normalized by the mean of the data.

Water levels were measured inside the Arcachon Lagoon (Figure 9) and the storm surge was computed as the difference between the observations and a tidal prediction based on a harmonic analysis performed over a 5-year time series using U-Tide (Codiga, 2011). For the model, the storm surge was computed as the difference between simulations including tides and surge and a simulation that is forced only by tides. The comparison between observed and modeled storm surges reveals firstly that without wave forces, the model underestimates the surge peak by a factor of 3. When short waves are included in the simulation, this strong negative bias is cancelled out and the RMSE is reduced by a factor of 3 (Figure 9). For the total water level, including short waves also removes a 0.27 m negative bias and reduces the RMSE by a factor of 3. This behavior was already observed by Lavaud et al. (2020), for the storm Klaus (2009), and explained by the dissipation of storm waves at the entrance of the Arcachon Lagoon, which drives a large wave setup that extends at the scale of the whole lagoon. This new application demonstrates that the results of Lavaud et al. (2020) were not specific to a particular storm and suggest that short waves should be included in storm surge forecasts when intense wave breaking occurs at the entrance of estuaries and lagoons.

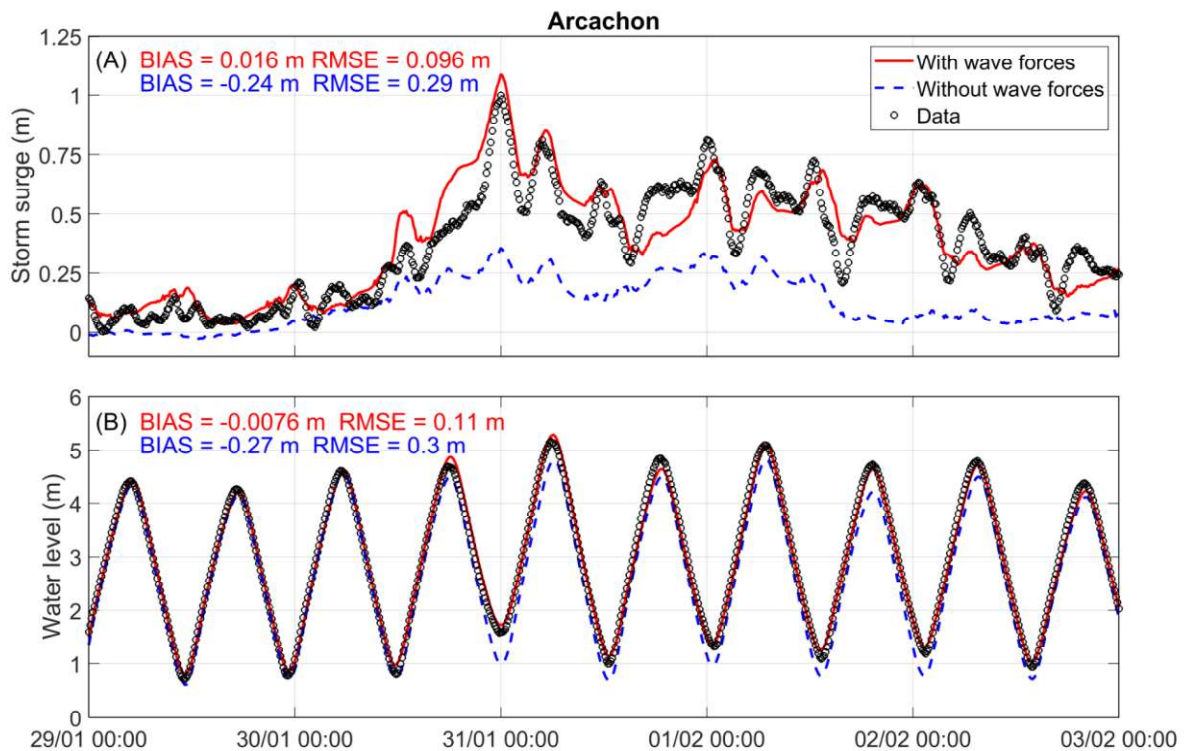


Figure 9. (A) Observed (black circles) against modeled storm surge with (blue) and without (red) short waves and (B) same for total water levels.

3.3. Impacts of bathymetric changes on forecasted nearshore circulation at Figueira da Foz

3.3.1. Motivation and goals

In nearshore areas, short-term predictions of coastal hydrodynamics are useful for harbor navigation, bathing safety and civil protection. Because these areas are shallow, the hydrodynamic conditions can be affected by bathymetric changes. These changes can occur rapidly due to both natural and anthropogenic causes, such as storm-driven erosion or dredging and deposition. Thus, the accuracy of model predictions could depend on frequent updates of the bathymetry.

To assess this dependence, sensitivity tests to observed bathymetric evolutions were performed near a jettied tidal inlet on the western coast of Portugal. These tests were made using an OPENCoastS forecast, and illustrate how the platform can be exploited for hindcast runs. Indeed, these hindcast runs were done using the input files created and made available through the forecast runs. The forecast was initially implemented for the nearshore area in the vicinity of the harbor of Figueira da Foz (Figure 10a), following the 2D W&C workflow (Figure 2). The unstructured grid has about 50,000 nodes and extends from 84 m water depth offshore to 14 km upstream the Mondego estuary; the grid spatial resolution ranged from 2.5 km offshore to 20 m in the nearshore area and along stream, and the timestep was set to 30 seconds. The forecast system (Nahon et al., 2020) was implemented in OPENCoastS with a bathymetry surveyed in the summer 2019 (ebb-tidal delta and subtidal sandbars) and March 2020 (intertidal beach). The model skill is evaluated for offshore and nearshore significant wave height, and nearshore, harbor and river water level elevation and is summarized in Table 3.

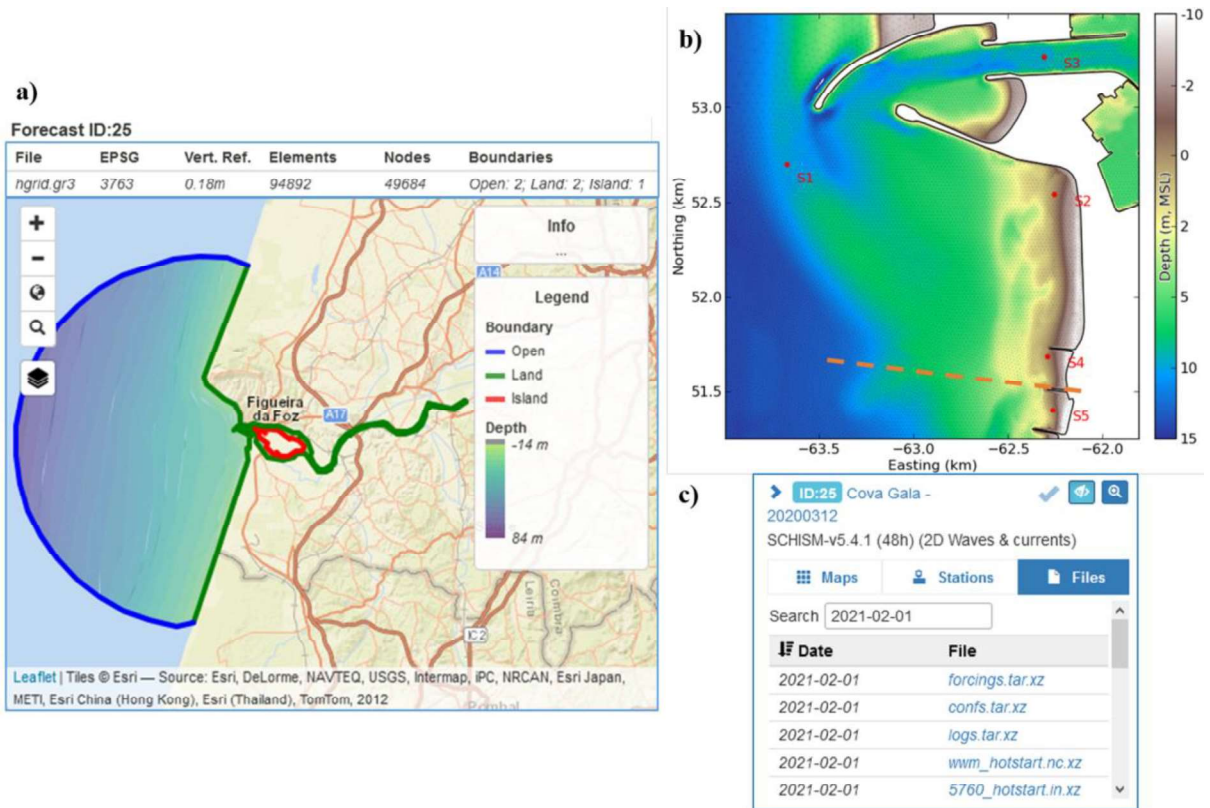


Figure 10. Figueira da Foz Forecast system: a) computational domain as seen in OPENCoastS; b) Cova Gala Beach, south of the harbor entrance, with the location of the output stations (S1-S5) and of the bathymetric profile shown in Figure 11a (dashed orange line); c) OPENCoastS tool to download daily files containing forcings, hotstarts and model results.

Table 3. Bias and root mean square errors (RMSE) between modeled and observed significant wave height (H_s) and water level elevation across the computational domain (after Nahon et al., 2020)

	Hs		Elevation	
	Bias (% of mean)	RMSE (% of mean)	Bias (m)	RMSE (m)
Offshore: Wave buoy	-13.4	20.4	-	-
Nearshore: Pressure transducers	-17.3 < . < 12.4	13.9 < . < 20.0	0.13 < . < 0.26	0.14 < . < 0.26
Harbor: Tidal gauge	-	-	-0.01	0.04
Upstream: Tidal gauge	-	-	-0.07	0.12

3.3.2. Measured bathymetric changes

The sensitivity of the model results to the bathymetry was assessed considering two bathymetries in addition to the one from 2019/20 used in the forecast system. The first bathymetry was used to investigate the consequence of the inflow of sediments from the beach and sandbars to the north of the inlet's northern jetty. During storms, this inflow of sediments can rapidly accrete the access channel (S1 location, Figure 10b), as, for example, during the storm Epsilon in October 2020 (Figure 11b). A post-Epsilon survey, made on 6 November 2020, was then used to modify the reference bathymetry and assess the impacts on waves and current predictions.

In recent years, the sand brought in by (storm) waves is dredged and deposited in front of Cova Gala Beach, to the south of the inlet's southern jetty. In 2018, these deposits created a protuberance of the ebb-tidal delta. Initially within 6 m to 10 m depth (chart datum), the deposit subsequently spread and evolved into large nearshore sandbars visible in the 2019 bathymetry (Figure 11a). In the second bathymetry, the nearshore area was changed to a state representative of summer 2018.

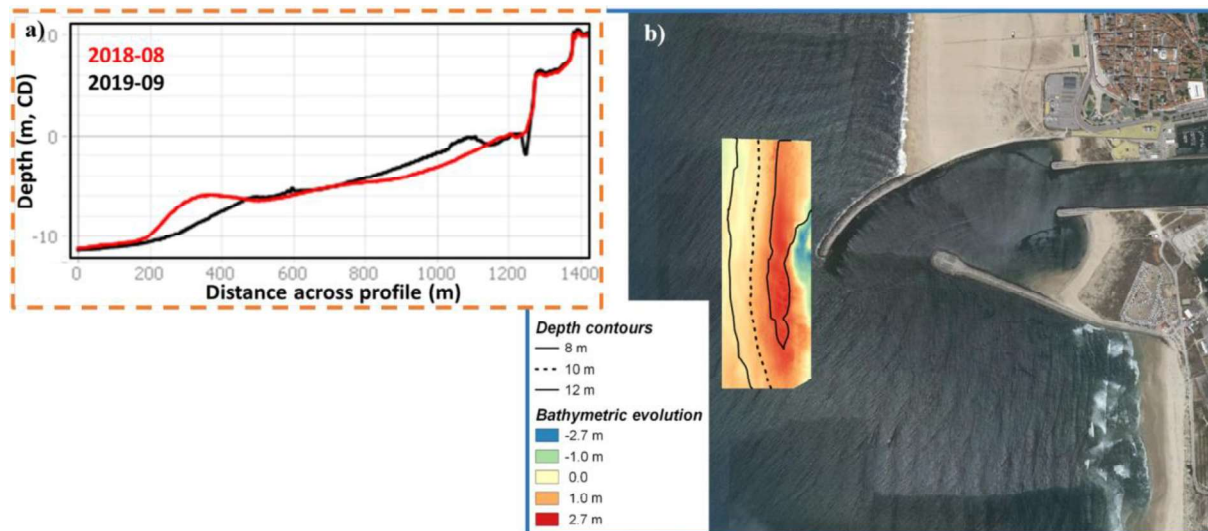


Figure 11. Bathymetric evolution near Figueira da Foz harbor: a) bathymetric evolution of the 2018 dredging disposal (red) through to 2019 (black), along the profile plotted on Figure 10b (dashed orange line); b) bathymetric evolution of the harbor entrance channel during storm Epsilon (October, 2020) along with post-storm depth contours (positive is accretion).

3.3.3. Duplicated forecasts and hydrodynamic results

All input files and forcings were downloaded from the OPENCoastS service web app using the Files download tool accessible within the Outputs viewer (Figure 10c): input files from 1 February 2021 were used with circulation initial conditions created on 31 January 2021. The model was then run offline for the three bathymetric configurations.

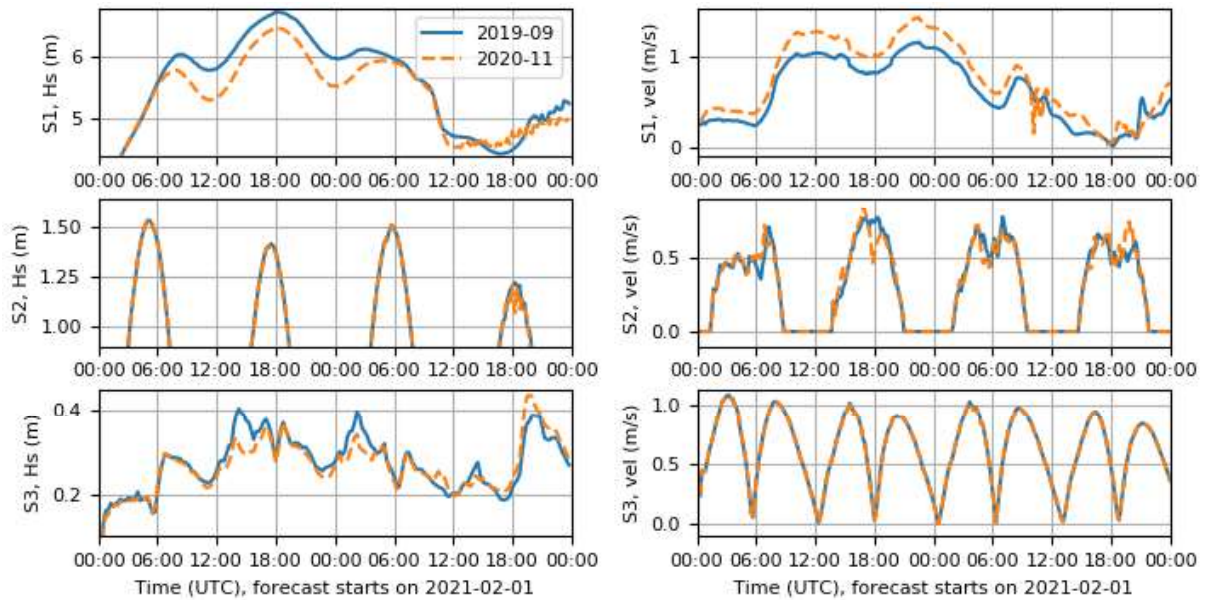
Simulations were analyzed at five virtual output stations (Figure 10b), although here results were outputted every 10 min compared to 1 hour outputs within OPENCoastS. Stations S1-S3 were placed to evaluate the sensitivity of the harbor hydrodynamics to bathymetric changes induced by storm Epsilon. Stations S4-S5 were placed shoreward of the 2018 sediment disposal location to analyze the impact of the dredging spoils on the beach hydrodynamics.

The simulated period covered the 2nd storm modeled in the previous case study in the Bay of Biscay. Here, the offshore significant wave height peaked at 6.9 m at 15:00 on 1 February, before the high tide of a moderate 2.5 m tidal cycle. At stations S1-S3, the main differences concerned the significant wave height and the current velocities, and were largest within the access channel (S1, Figure 12). At S1, compared to the configuration with a well-defined channel, the post-storm configuration showed a modest decrease of 5% of the significant wave height at the peak of the storm and a stronger increase of the current velocities, on the order of 20%. Differences at the beach (S2, 0 m depth MSL) are less pronounced, likely because the surfzone was saturated and the wave height was controlled by the depth-induced breaking. In the 9-m deep main harbor channel (S3), differences in velocities were negligible. In contrast, the wave height was affected by up to 25% although this concerned waves with a modest size. However, phase-averaged models such as WWM only provide an approximate representation of wave diffraction which may limit the accuracy of the wave predictions between the jetties. Also, WWM does not reproduce the wave reflection at the jetties.

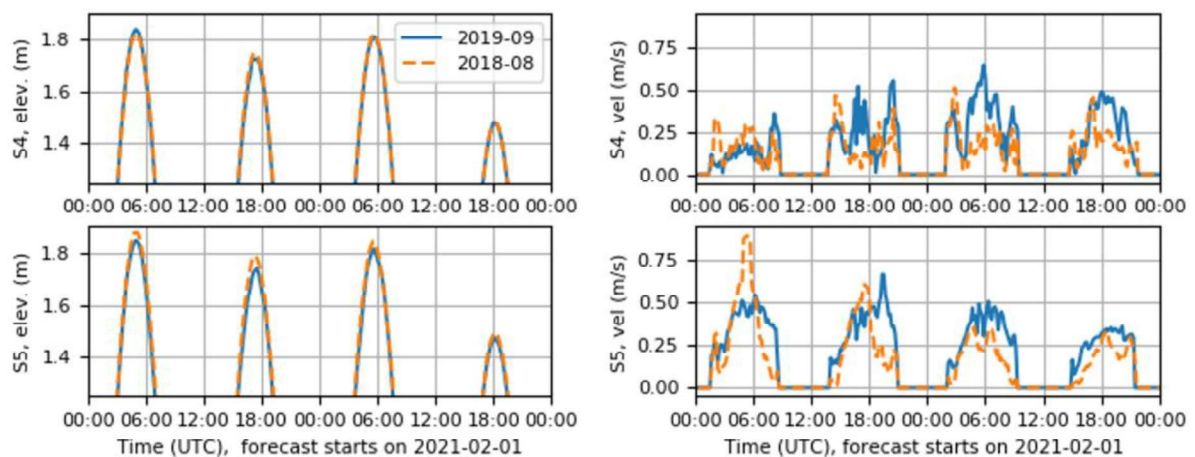
Stations S4-S5 were placed along the 0 m depth contour, southward of the tidal inlet. Similarly to S2, differences in significant wave height were negligible. Differences in total water level reached 5 cm (Figure 13). The main differences at those beach cells were observed in the intensity of the modeled current, with overall stronger currents, after the deposited sediment migrates shoreward (2019-09 configuration).

Overall, these results show that, although the bathymetric changes were significant, differences were modest in terms of modeled significant wave

1 height and total water levels. The main differences occurred for the predicted
 2 current velocities in the access channel (S1) and over the intertidal beach in the
 3 shadow of the dredging spoils (S4 and S5). However, these results cannot be
 4 generalized since this analysis was made under specific wave and tidal
 5 conditions.
 6
 7



8
 9
 10
 11
 12
 13
 14
 15
 16
 17
 18
 19
 20
 21
 22
 23
 24
 25
 26
 27
 28 Figure 12. Sensitivity of the significant wave height (Hs, left) and current
 29 velocities (right) to storm-driven bathymetric evolutions in late October 2020.
 30
 31
 32



33
 34
 35
 36
 37
 38
 39
 40
 41
 42
 43
 44
 45
 46
 47
 48
 49
 50
 51
 52
 53
 54
 55
 56
 57
 58
 59
 60
 61
 62
 63
 64
 65

Figure 13. Sensitivity of nearshore water levels (left) and current velocities (right) to bathymetric evolutions following the disposal of dredging material in 2018.

3.4. Tagus estuary 3D baroclinic case study

1 The Tagus estuary (Portugal) is one of the largest estuaries in Europe and holds
2 a major natural reserve, which is one of the most important sanctuaries for
3 wintering or staging birds. The estuarine margins are intensively occupied, with
4 a population of about one million inhabitants, and support diverse uses and
5 activities (urban, industrial/harbors, agriculture, shellfish harvesting). The
6 estuary has a deep and narrow inlet channel and a broad and shallow inner
7 basin. The intertidal area constitutes about 40% of the total estuarine surface
8 (Castanheiro, 1986). Tides are the main driver of the circulation in the Tagus
9 estuary (Fortunato et al., 2017b). Tides are semi-diurnal and range from 0.55 m
10 to 3.86 m at the coast (Guerreiro et al., 2015). The tidal propagation within the
11 estuary is complex and tidal amplitudes are amplified by resonance (Fortunato
12 et al., 1997, 1999). Other drivers, such as the river flow, wind, atmospheric
13 pressure and surface waves, also influence the circulation within the estuary.
14 The Tagus River, with an average flow of 370 m³/s (APA, 2012), is the main
15 source of freshwater into the estuary. Other tributaries (the Sorraia and the
16 Trancão rivers) also contribute to the freshwater inflow into the estuary. The
17 estuary is usually well-mixed, but stratification can occur at high flow rates and
18 low tidal ranges (Neves, 2010; Rodrigues and Fortunato, 2017). Residence
19 times in the estuary result from the interaction between different factors, such as
20 tide, river flow and wind (e.g., Oliveira and Baptista, 1997; Vaz and Dias,
21 2014). Several studies showed the interaction between the Tagus and the
22 adjacent coastal area and the sediments, nutrients, plankton and fisheries
23 dynamics in the estuary (e.g., Gameiro and Brotas, 2010; Valente and Silva,
24 2009). The physical drivers play an important role in these dynamics. In the
25 Tagus estuary, residence time is the main factor influencing phytoplankton
26 annual variability (Brotas and Gameiro, 2009), with lower concentrations
27 occurring during wet years. Moreover, other physical factors, such as salinity
28 can influence the biotic distribution within the estuaries (e.g. Wolf et al., 2009).
29 The operational model of the Tagus estuary was first implemented and validated
30 in hindcast mode (Rodrigues and Fortunato, 2017). The model extends from the
31 ocean to the river and the domain is discretized with a horizontal grid of
32 about 83,000 nodes and 157000 elements, which has a typical resolution of 15-
33 25 m (Figure 14). The vertical domain is discretized with a hybrid grid with 39
34 SZ levels (30 S levels in the upper 100 m, and 9 Z levels between 100 m and the
35 maximum depth). Within OPENCoastS (Figure 15) the model is forced by: i)
36 sea surface heights, salinity, water temperature from the CMEMS-IBI model at
37 the oceanic boundary; ii) extrapolation of river flows from the SNIRH Almourol
38
39
40
41
42
43
44
45
46
47
48
49
50
51
52
53
54
55
56
57
58
59
60
61
62
63
64
65

station (<http://snirh.apambiente.pt>), zero salinity and monthly climatological values of water temperature at the riverine boundaries (Tagus and Sorraia rivers); and iii) atmospheric data at the surface from the GFS model. The time step was set to 30s.

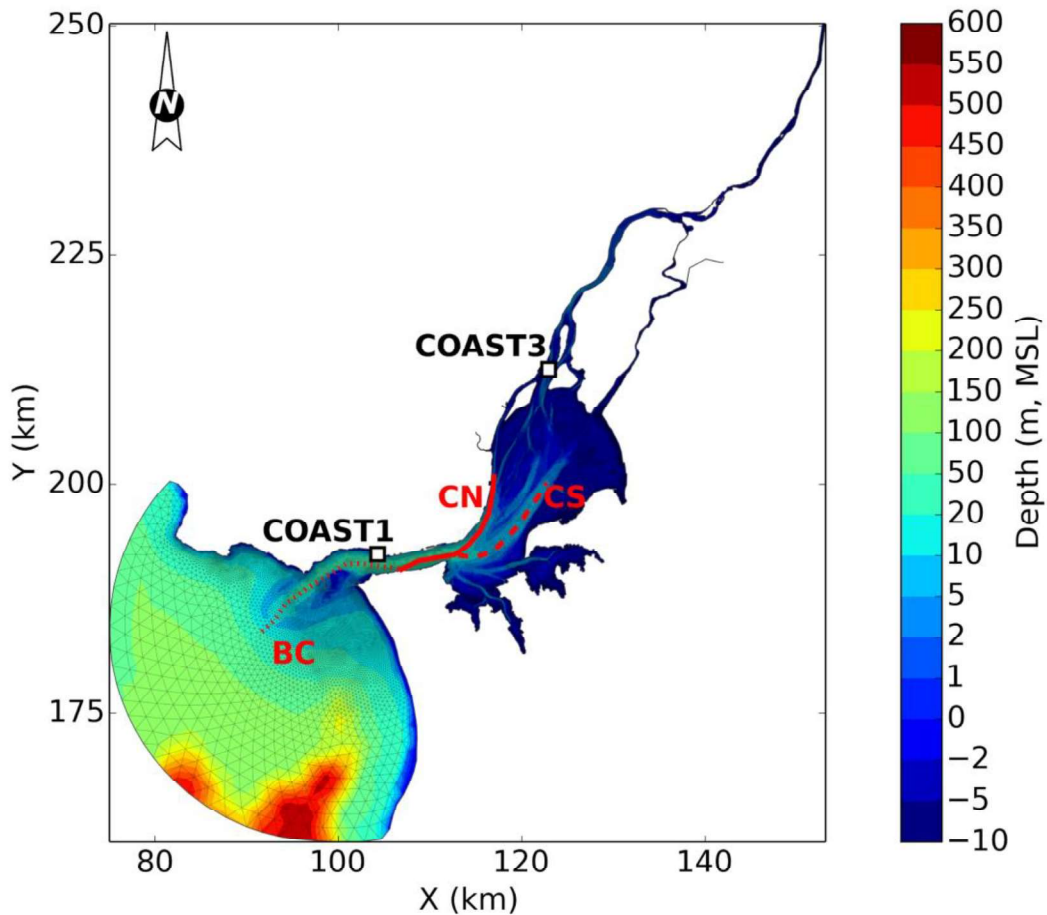


Figure 14. Horizontal grid and location of the stations. The Almourol station, used to provide river boundary conditions, is located about 37 km upstream of the model domain

Data from the COASTNET Portuguese monitoring network (<http://geoportal.coastnet.pt/>) were used to assess the operational model salinity and water temperature. The data-model comparison was performed between November 2019 and February 2020, which includes a period of high river flows susceptible to lead to stratification (Rodrigues and Fortunato, 2017), aiming to assess the operational model response for different forcing conditions.

Results show the ability of the model to represent the main variations regarding salinity and water temperature, both upstream and downstream (Figure 16,

1 supplementary material #2). However, the temperature is underestimated
2 upstream, where a negative bias is observed (Figure 16, supplementary material
3 #2). RMSE and mean absolute error (MAE) for salinity and water temperature
4 (Figure 16) are typically of the same order of magnitude of previous hindcast
5 applications (Rodrigues and Fortunato, 2017; Rodrigues et al., 2019), although
6 slightly higher upstream. The differences observed between the data and the
7 model forecasts may be due to the boundary conditions imposed. At the riverine
8 boundaries, the river flow is extrapolated from the last flow measured, which
9 may introduce phase errors in the model results (of about 1-2 days) when
10 significant variations of the flow occur. Also, the water temperature at these
11 boundaries is based on climatology, which constitutes a major source of
12 uncertainty and may explain the larger differences observed in the upstream
13 station. The atmospheric forcing may also influence the salinity and water
14 temperature dynamics in the Tagus estuary (Rodrigues et al., 2016 and
15 Rodrigues and Fortunato, 2017) and explain some of the differences observed,
16 since a global model with a low resolution was used.

17
18
19
20
21
22
23
24
25
26 The 3D model is able to represent the vertical dynamics of salinity and water
27 temperature in the Tagus estuary, which is expected to become stratified for
28 river flows higher than 1000 m³/s. The operational model represents the
29 stratified conditions (Figure 17 and Figure 18) that occur during a period where
30 river flow was about 2000 m³/s. Results show that the riverine plume extends
31 further into the ocean for larger river flows and leads to the stratification of the
32 water column, with salinities near the inlet of about 20 at the surface and about
33 32-34 near the bottom at low tide. For a river flow of about 370 m³/s (close to
34 the mean river flow of the Tagus river - 360 m³/s) the mixing is stronger; near
35 the inlet salinity ranges between 30-34 at low tide.

36
37
38
39
40
41
42 Overall the forecasts proved to adequately represent the salinity and water
43 temperature dynamics in the Tagus estuary and can provide useful information
44 to support diverse activities in the area.
45
46
47
48
49
50
51
52
53
54
55
56
57
58
59
60
61
62
63
64
65

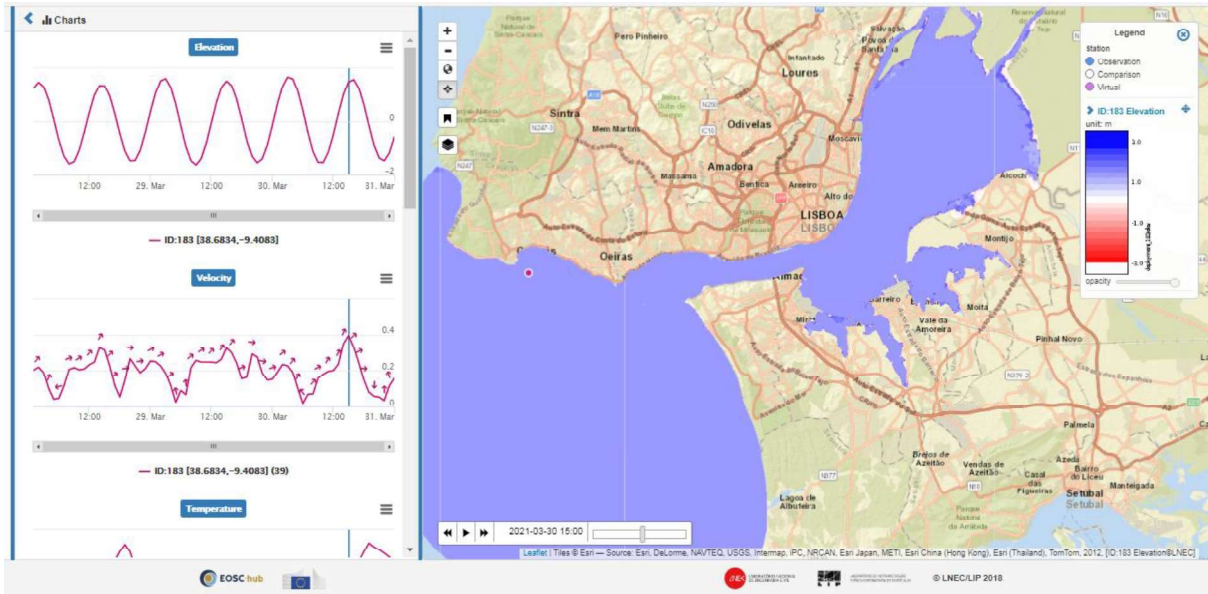


Figure 15. Outputs viewer: Water levels and velocities at Cascais - Tagus estuary. The time series of water levels and velocities on the left were extracted at the red circle outside the mouth.

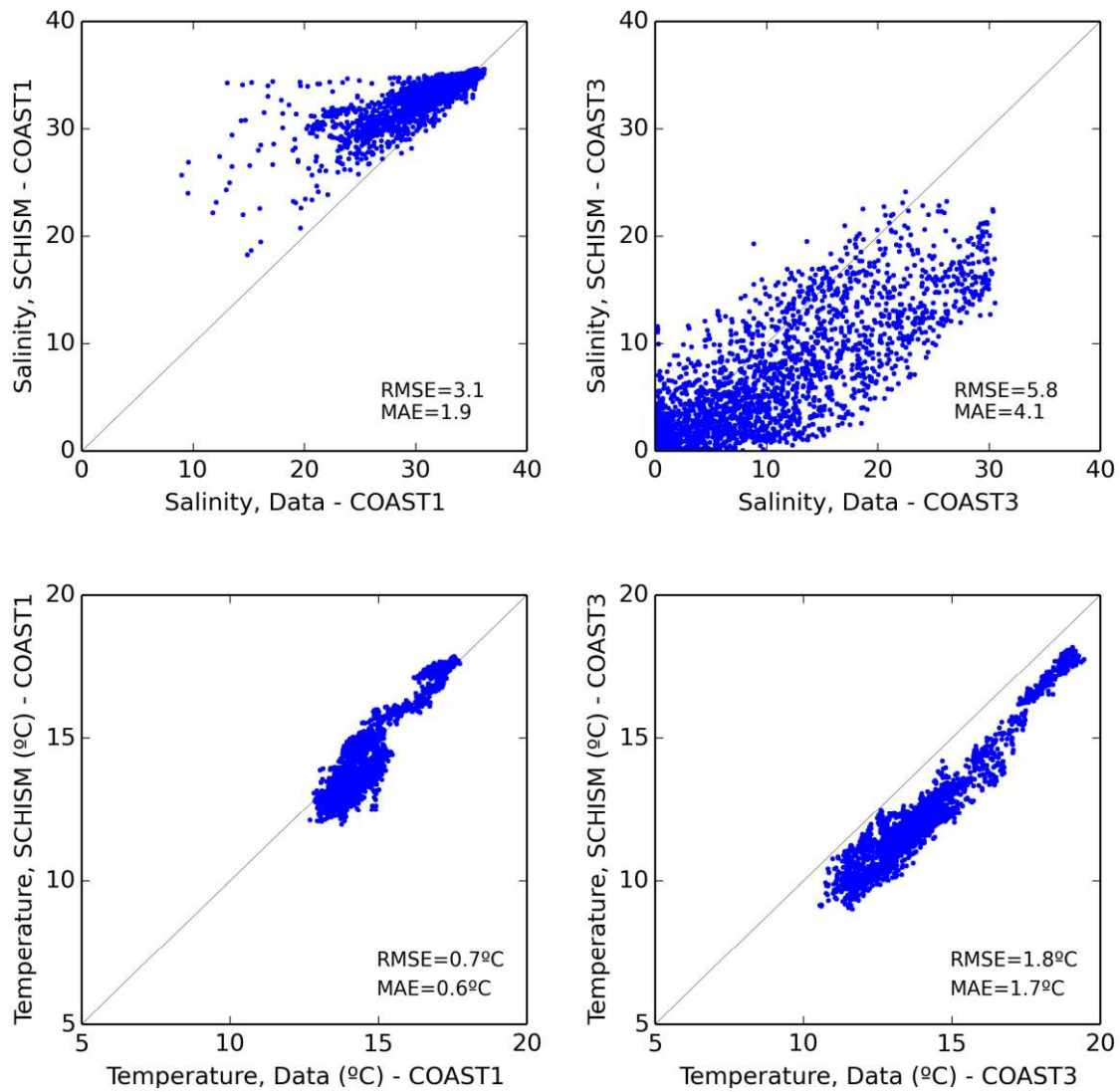
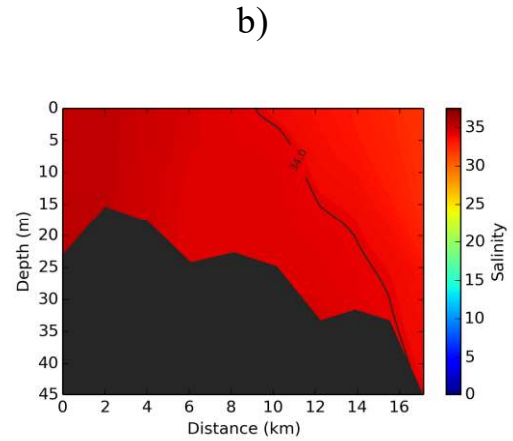
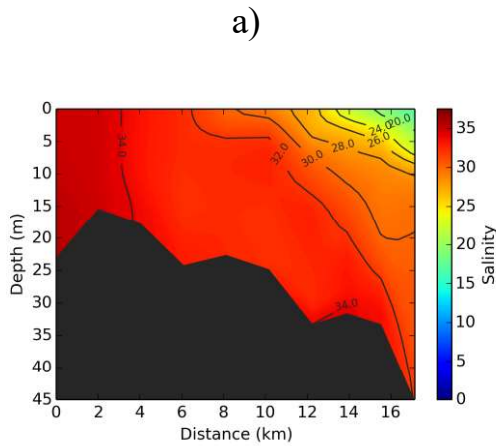
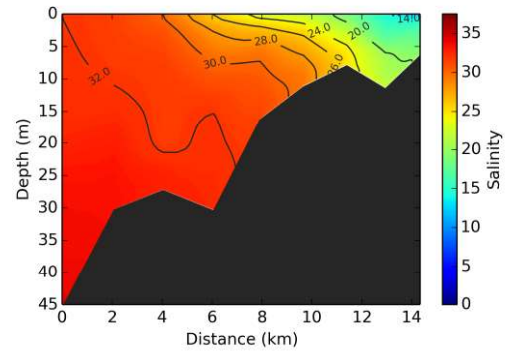
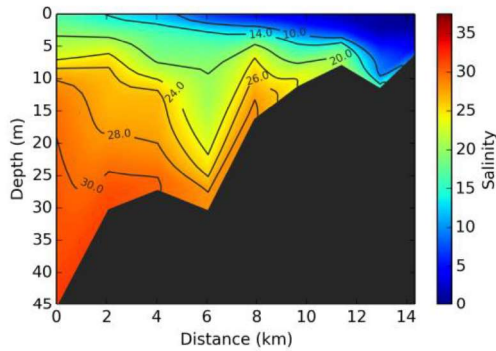


Figure 16. Salinity and water temperature data vs SCHISM Forecasts in the Tagus estuary. Root mean square error (RMSE) and mean absolute error (MAE) for salinity and water temperature are indicated in the figures.

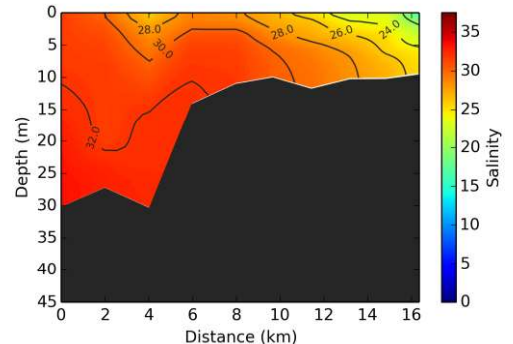
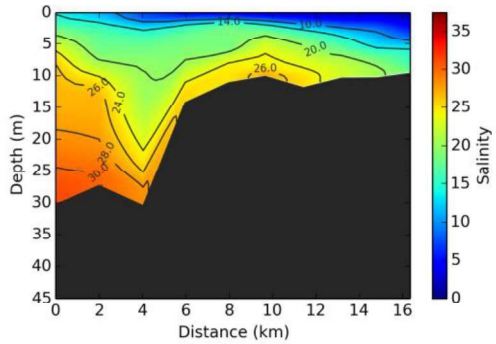
1
2
3 Barra-
4 Corred
5 or
6
7
8
9



16
17 Cala do
18 Norte
19
20
21
22
23
24
25
26
27

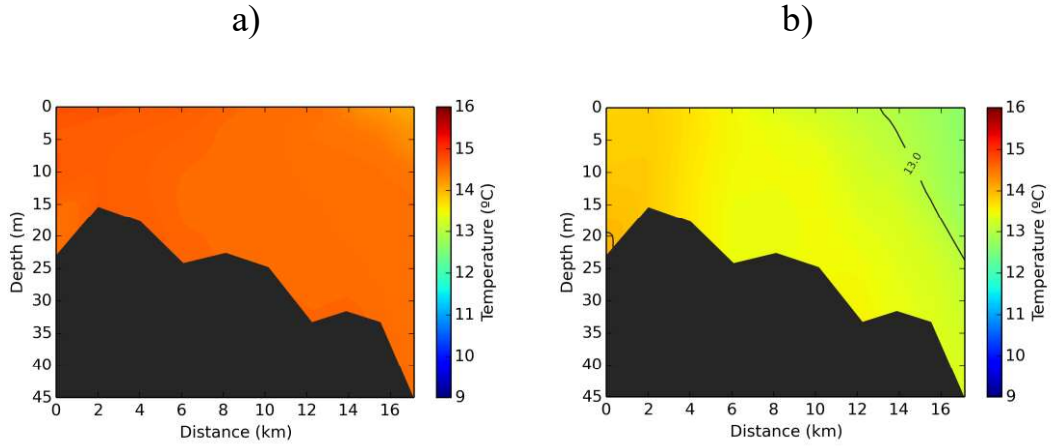


30
31 Cala de
32 Samora
33
34
35
36
37
38
39
40
41
42
43
44

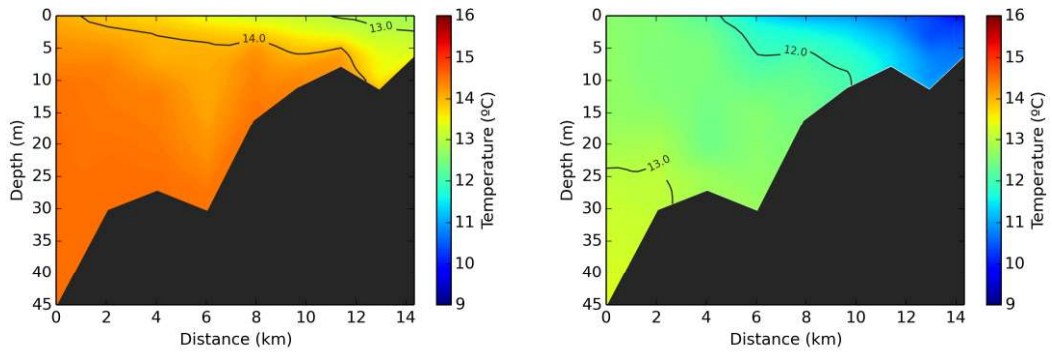


45
46 Figure 17. Forecasted vertical profiles of salinity at low tide on a) December 23,
47 2019 - estimated river flow of 2000 m³/s and b) January 25, 2020 - estimated
48 river flow of 370 m³/s (see Figure 14 for the location of the longitudinal
49 profiles).
50
51
52
53
54
55
56
57
58
59
60
61
62
63
64
65

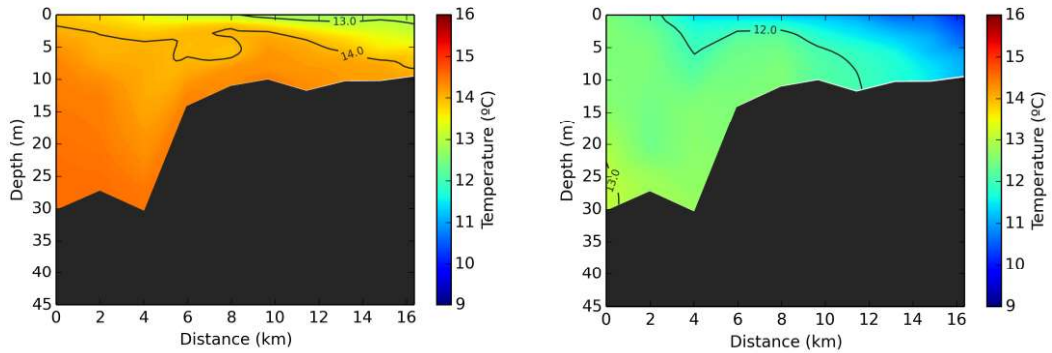
1
2
3 Barra-
4 Corred
5 or
6
7
8
9



16
17 Cala do
18 Norte
19
20
21
22
23
24
25
26
27



28
29
30
31 Cala de
32 Samora
33
34
35
36
37
38
39
40
41
42
43
44



45
46 Figure 18. Forecasted vertical profiles of water temperature on December 23,
47 2019 and on January 25, 2020, at low tide (see Figure 14 for the location of the
48 longitudinal profiles).
49
50
51
52
53
54
55
56
57
58
59
60
61
62
63
64
65

4. Discussion, conclusions and future perspectives

Over the past three years, OPENCoastS has grown from an innovative on-demand platform that addressed simple 2D barotropic forecasts to a powerful tool that solves all circulation options, used by over 400 users and applied on all continents. Most past applications are scientific ones, to understand the importance of processes at a site or to explore the influence of numerical and physical parameters or forcing sources on forecasts, among other goals. Several deployments were also built to predict site circulation, either to support field work preparation or to anticipate hazardous conditions.

The applications presented herein proved the usefulness of OPENCoastS and provided important lessons. The application to the coast of Taiwan showed that useful forecasts can be obtained using only large-scale public data. This success is very important, considering the existence of many data-poor environments worldwide without forecast systems. Also, this forecast was run with simplified physics (i.e., waves were neglected). Although this simplification is still common in forecast systems (Umgiesser et al., in press), waves can play an important role in the storm surge (Lavaud et al., 2020; Liu and Huang, 2020). This role is confirmed in the Bay of Biscay application, where the inclusion of wave forces reduces the error in the storm surge by a factor of 3. To a smaller extent, the accuracy of the forecasts in shallow areas also depends on accurate and updated bathymetries. This dependence is illustrated in the Figueira da Foz harbor example. The limitations imposed by the lack of detailed data is also highlighted in the Tagus Estuary case, which suggests that absence of small-scale atmospheric predictions and river flow forecasts constitute important sources of errors. In summary, while OPENCoastS can provide useful results using only publicly available data and simplified physics, the more demanding users should include high-resolution and updated data, and include all the relevant processes. The possibility to use atmospheric predictions provided by the user is planned for future versions of OPENCoastS, similar to the current capacity to specify a source for river flow predictions.

The applications presented herein also highlight the usefulness of OPENCoastS as a tool to automate many time-consuming tasks in coastal modeling, such as the generation of input files, downloading and processing of atmospheric forecast and post-processing of model results. This automation fosters the use of models for sensitivity analyses, as illustrated by the Bay of Biscay application.

1 Although OPENCoastS was designed to generate forecasts, the Figueira da Foz
2 harbor application shows how it can be exploited for hindcasts, taking
3 advantage of the automatic generation of input files.
4

5
6 In spite of OPENCoastS only requiring an unstructured computational grid to
7 set up a new forecast, the availability of such grids remains a limitation for
8 many users, in particular for those outside the academic fora. Recent
9 developments in automatic grid generation (e.g., Roberts et al., 2019), along
10 with the availability of global bathymetry services, have paved the way for an
11 integration of a grid generator in the configuration assistant of OPENCoastS.
12 The robustness of the computational engine SCHISM, even for highly skewed
13 grids and noisy bathymetries, is paramount for the success of this task, bearing
14 in mind the need to include the necessary grid features for a good simulation,
15 depending on the simulation type (e.g. good representation of the channel cross-
16 sections and dikes).
17
18
19
20
21
22
23
24

25 While forecasts are often much more difficult to build than simple offline
26 applications of a specific model, thus justifying the development of
27 sophisticated on-demand platforms such as OPENCoastS, these two tasks share
28 a common need in high-resolution runs. These runs can be either for
29 applications to very large domains (regional or global modeling), spatially very
30 small events (e.g. discharge of an outfall) or multiple runs (e.g. scenarios
31 simulation), but they all require very large computational resources. Moreover,
32 a user-friendly platform may significantly reduce the learning curve on how to
33 use a new model and to build on-the-fly boundary conditions from several
34 sources. Therefore, hincast or scenario simulations are now being integrated in
35 OPENCoastS, supported by atmospheric reanalyses and FES2014,
36 complemented by the inverse barometer effect.
37
38
39
40
41
42
43
44
45

46 The integration of hindcast simulations in OPENCoastS raises an important
47 issue on the evaluation of the quality of those runs. A small level of in-situ data
48 was integrated in the platform, supported by the extensive network of
49 EMODNET physics' water level stations and by processing Sentinel images for
50 water/land interface detection. However, much remains to be done regarding the
51 evaluation of salinity and temperature, waves and velocities. Better exploitation
52 of remote sensing either from satellites (for temperature, salinity and wave
53 comparisons) or radar networks (for surface velocities) will be considered along
54 with a more extensive usage of EMODNET data for the same variables.
55
56
57
58
59
60
61
62
63
64
65

1
2
3
4
5
6
7
8
9
10
11
12
13
14
15
16
17
18
19
20
21
22
23
24
25
26
27
28
29
30
31
32
33
34
35
36
37
38
39
40
41
42
43
44
45
46
47
48
49
50
51
52
53
54
55
56
57
58
59
60
61
62
63
64
65

Finally, the current implementation of OPENCoastS in EOSC should also be improved to allow for better multisite scalability, elasticity, high availability and redundancy to guarantee services operation. The goals are to improve data movement between hosting infrastructure sites, using the EGI Data Transfer, and automation, scalability and elasticity using Infrastructure Manager and EGI Cloud Container Compute. Moreover, this approach will also provide an improved deployment of a distributed database solution, so that all available OPENCoastS infrastructure providers can be used transparently. This solution targets the guarantee of optimized and timely delivery of service which is fundamental for quality assurance of operational forecast systems and its high demand for immediate access to the computational resources.

Acknowledgements

This work was funded by the European Commission through the H2020 projects EOSC-hub (Grant Agreement No 777536) and EOSC-Synergy (Grant Agreement No 857647), by Lisboa2020 Operational Program through the INCD project (LISBOA-01-0145-FEDER-022153) and by the Fundação para a Ciência e a Tecnologia through projects MOSAIC.pt (PTDC/CTA-AMB/28909/2017) and AQUAMON (PTDC/CCI-COM/30142/2017). This work made use of results produced with the support of the Portuguese National Grid Initiative; more information in <https://wiki.ncg.ingrid.pt>.

The test cases of Figueira da Foz Harbor were made thanks to bathymetric data made available by the Coastal Monitoring Programme of Continental Portugal - COSMO, co-funded within POSEUR-09-2015-25, and thanks to bathymetric data obtained within the project NAVSAFETY, funded by the Direção-Geral de Política do Mar, in the scope of the Fundo Azul.

References

- Allan, J., Priest, G.R., Zhang, Y.J. and Gabel, L. (2018). Maritime tsunami evacuation guidelines for the Pacific Northwest coast of Oregon. *Natural Hazards*, 94, 21–52. <https://doi.org/10.1007/s11069-018-3372-2>
- APA – Agência Portuguesa do Ambiente (2012) *Plano de Gestão da Região Hidrográfica do Tejo, Relatório Técnico – Síntese*. Ministério da Agricultura, do Mar, do Ambiente e do Ordenamento do Território.

- 1
2
3
4
5
6
7
8
9
10
11
12
13
14
15
16
17
18
19
20
21
22
23
24
25
26
27
28
29
30
31
32
33
34
35
36
37
38
39
40
41
42
43
44
45
46
47
48
49
50
51
52
53
54
55
56
57
58
59
60
61
62
63
64
65
- Bedri, Z., A. Corkery, J.J. O'Sullivan, M.X. Alvarez, A.C. Erichsen, L.A. Deering, K. Demeter, G.M.P. O'Hare, W.G. Meijer, B. Masterson (2014). An integrated catchment-coastal modelling system for real-time water quality forecasts, *Environmental Modelling & Software*, 61, 458-476. DOI: 10.1016/j.envsoft.2014.02.006
- Bertin, X., Li, K., Roland, A., Zhang, Y. J., Breilh, J. F., & Chaumillon, E. (2014). A modeling-based analysis of the flooding associated with Xynthia, central Bay of Biscay. *Coastal Engineering*, 94, 80-89. DOI: 10.1016/j.coastaleng.2014.08.013
- Bertin, X., Li, K., Roland, A., & Bidlot, J. R. (2015). The contribution of short-waves in storm surges: Two case studies in the Bay of Biscay. *Continental Shelf Research*, 96, 1-15. DOI: 10.1016/j.csr.2015.01.005
- Brevik, O., A.A. Allen, 2008. An operational search and rescue model for the Norwegian Sea and the North Sea, *Journal of Marine Systems*, 69/1-2: 99-113. DOI: 10.1016/j.jmarsys.2007.02.010
- Brotas V., Gameiro C. (2009). Padrões de variabilidade sazonal e interanual de nutrientes e fitoplâncton no estuário do Tejo. Plano de Ordenamento do Estuário do Tejo, Saberes e Reflexões. Gabinete de Ordenamento do Território, Administração da Região Hidrográfica do Tejo, Ministério do Ambiente, do Ordenamento do Território e do Desenvolvimento Regional, 150-153.
- Castanheiro, J.M. (1986). Distribution, transport and sedimentation of suspended matter in the Tejo Estuary. In *Estuarine processes: An application to the Tagus Estuary*; Secretaria de Estado do Ambiente e Recursos Naturais: Lisboa, Portugal, pp. 75–90.
- Chen, C., Robert C. Beardsley, Richard A Luetlich Jr., Joannes J. Westerink, Harry Wang, Will Perrie, Qichun Xu, Aaron S. Donahue, Jianhua Qi, Huichan Lin, Liuzhi Zhao, Patrick C. Kerr, Yanqiu Meng, Bash Toulany (2013). Extratropical storm inundation testbed: Intermodel comparisons in Scituate, Massachusetts, *J. Geophys. Res. Oceans*, 118, 5054-5073, doi:10.1002/jgrc.20397.
- Chiu, C., Huang, C., Wu, L., Zhang, Y., Chuang, L., Fan, Y., Yu, H-C. (2018) Forecasting of oil-spill trajectories by using SCHISM and X-band radar, *Marine Pollution Bulletin*, 137, 566-581.
- Codiga, D.L. (2011). *Unified Tidal Analysis and Prediction Using the Utide Matlab Functions*. Graduate School of Oceanography, University of Rhode Island Narragansett, RI.

- 1 Du, J., Park, K., Shen, J., Zhang, Y. J., Yu, X., Ye, F., Wang, Z., Rabalais, N.
2 N. (2019). A hydrodynamic model for Galveston Bay and the shelf in the
3 northern Gulf of Mexico, *Ocean Sciences*, 15, 951-966,
4 <https://doi.org/10.5194/os-15-951-2019>
5
- 6 Elsner, J.B., K.-B. Liu (2003). Examining the ENSO-Typhoon Hypothesis,
7 *Climate Research*. 25, 43. DOI:10.3354/cr025043
8
- 9 Fernandez-Montblanc, T., M.I. Vousedoukas, P. Ciavola, E. Voukouvalas, L.
10 Mentaschi, G. Breyiannis, L. Feyen, P. Salamon, (2019). Towards robust
11 pan-European storm surge forecasting, *Ocean Modelling*, 133, 129-144,
12 <https://doi.org/10.1016/j.ocemod.2018.12.001>.
13
- 14 Ferrarin, C., Davolio, S., Bellafiore, D., Ghezzi, M., Maicu, F., Mc Kiver, W.,
15 Drofa, O., Umgiesser, G., Bajo, M., De Pascalis, F., Malguzzi, P., Zaggia,
16 L., Lorenzetti, G., Manf, G. (2019). Cross-scale operational
17 oceanography in the Adriatic Sea, *Journal of Operational Oceanography*,
18 DOI: 10.1080/1755876X.2019.1576275
19
- 20 Fortunato, A.B; Bruneau, N.; Azevedo, A.; Araújo, M.A.V.C.; Oliveira, A.
21 (2011). Automatic improvement of unstructured grids for coastal
22 simulations, *Journal of Coastal Research*, Special Issue 64: 1028 – 1032.
23
- 24 Fortunato, A.B., Oliveira, A., Rogeiro, J., Tavares da Costa, R., Gomes, J.L., Li,
25 K., Jesus, G., Freire, P., Rilo, A., Mendes, A., Rodrigues, M., Azevedo A.
26 (2017a). Operational forecast framework applied to extreme sea levels at
27 regional and local scales. *Journal of Operational Oceanography*. 10(1),
28 1-15. doi:10.1080/1755876X.2016.1255471.
29
- 30 Fortunato, A.B., Freire, P., Bertin, X., Rodrigues, M., Ferreira, J., Liberato,
31 M.L.R. (2017b). A numerical study of the February 15, 1941 storm in the
32 Tagus estuary. *Continental Shelf Research*. 144, 50-64.
33 doi:10.1016/j.csr.2017.06.023.
34
- 35 Fortunato AB, Baptista AM, Luettich Jr. RA (1997) A three-dimensional model
36 of tidal currents in the mouth of the Tagus Estuary. *Continental Shelf
37 Research* 17: 1689-1714.
38
- 39 Fortunato AB, Oliveira A, Baptista AM (1999) On the effect of tidal flats on the
40 hydrodynamics of the Tagus estuary. *Oceanol Acta*, 22, 31-44.
41
- 42 Gameiro, C., Brotas, V. (2010). Patterns of Phytoplankton Variability in the
43 Tagus Estuary (Portugal), *Estuaries and Coasts* 33, 311–323
44 <https://doi.org/10.1007/s12237-009-9194-4>.
45
- 46 Gomes, J., E. Bagnaschi, I. Campos, M. David, L. Alves, J. Martins, J. Pina, A.
47 López-García, P. Orviz (2018). Enabling rootless Linux Containers in
48
49
50
51
52
53
54
55
56
57
58
59
60
61
62
63
64
65

- 1 multi-user environments: The udocker tool, *Computer Physics*
2 *Communications*, 232, 84-97, <https://doi.org/10.1016/j.cpc.2018.05.021>.
- 3 Guérin, T., Bertin, X., Dodet, G. (2016). A numerical scheme for coastal
4 morphodynamic modelling on unstructured grids. *Ocean Modelling*. 104,
5 45-53. doi:10.1016/j.ocemod.2016.04.009.
- 6
7
8 Guerreiro, M., Fortunato, A.B., Freire, P., Rilo, A., Taborda, R., Freitas, M.C.,
9 Andrade, C., Silva, T., Rodrigues, M., Bertin, X., Azevedo, A. (2015).
10 Evolution of the hydrodynamics of the Tagus estuary (Portugal) in the
11 21st century. *Revista de Gestão Costeira Integrada*, 15, 65-80.
12 doi:10.5894/rgci515.
- 13
14
15
16 Huang, W., Ye, F., Zhang, Y., Park, K., Du, J., Moghimi, S., Myers, E., Pe'eri,
17 S., Calzada, J.R., Yu, H.C., Nunez, K., and Liu, Z. (2021) Compounding
18 factors for extreme flooding around Galveston Bay during Hurricane
19 Harvey, *Ocean Modelling*, 158, 101735.
- 20
21
22
23 Lavaud, L., Bertin, X., Martins, K., Arnaud, G., Bouin, M. (2020) The
24 contribution of short-wave breaking to storm surges: The case Klaus in
25 the Southern Bay of Biscay, *Ocean Modelling*, 156.
- 26
27
28 Li, X., Zhong, D., Zhang, Y., Wang, Y., Wang, Y., and Zhang, H. (2018) Wide
29 river or narrow river: Future river training strategy for Lower Yellow
30 River under global change, *International Journal of Sediment Research*,
31 <https://doi.org/10.1016/j.ijsrc.2018.04.001>
- 32
33
34
35 Liu, W.-C. ; Huang, W.-C., (2020). Investigating typhoon-induced storm surge
36 and waves in the coast of Taiwan using an integrally-coupled tide-surge-
37 wave model, *Ocean Engineering*, 107571, DOI:
38 10.1016/j.oceaneng.2020.107571.
- 39
40
41 Longuet-Higgins, M.S., Stewart, R. (1964). Radiation stresses in water waves; a
42 physical discussion, with applications. *Deep Sea Research and*
43 *Oceanographic Abstracts*, 11/ 4. 529–562.
- 44
45
46 Lyard, F.H., Allain, D.J., Cancet, M., Carrère, L., Picot, N. (2020). FES2014
47 global ocean tides atlas: design and performances, *Ocean Sciences*,
48 <https://os.copernicus.org/preprints/os-2020-96/>.
- 49
50
51 Lynett, P.J., Gately, K., Wilson, R., Montoya, L., Adams, L., Arcas, D., Aytore,
52 B., Bai, Y., Bricker, J.D., Castro, M.J., Cheung, K., David, C., Dogan, G.,
53 Escalante, C., Gonzalez, F.I., Gonzalez-Vida, J., Grilli, S.T., Heitmann,
54 T.W., Horrillo, J., KaÅnoÃ,,Ålu, U., Kian, R., Kirby, J.T., Li, W.,
55 Macaas, J., Nicolsky, D.J., Ortega, S., Pampell-Manis, A., Park, Y.,
56 Roeber, V., Sharghivand, N., Shelby, M., Shi, F., Tehranir, B., Tolkova,
57
58
59
60
61
62
63
64
65

- 1 E., Thio, H., Velioglu, D., Yalciner, A., Yamazaki, Y., Zaytsev, A.,
2 Zhang, Y. (2017) Inter-Model Analysis of Tsunami-Induced Coastal
3 Currents, *Ocean Modelling*, 114, 14-32
4
- 5 Nahon, A., Fortunato, A.B., Azevedo, A., Oliveira, F.S.B.F., Oliveira, J.N.C.,
6 Rogeiro, J., Jesus, G., Oliveira, A., Silva P.A., and Freire, P., 2020.
7 Implementation and validation of an operational forecasting system for
8 nearshore hydrodynamics with OPENCoastS. *Atas das 6as Jornadas de*
9 *Engenharia Hidrográfica / Ias Jornadas Luso-Espanholas de*
10 *Hidrografia*. 203-206, Instituto Hidrográfico, Lisboa
11
- 12 Neves FS (2010) *Dynamics and hydrology of the Tagus estuary: results from in*
13 *situ observations*. PhD Thesis, Universidade de Lisboa, Portugal.
14
- 15 Oke, Peter R., Roger Proctor, Uwe Rosebrock, Richard Brinkman, Madeleine L.
16 Cahill, Ian Coghlan, Prasanth Divakaran, Justin Freeman, Charitha
17 Pattiaratchi, Moninya Roughan, Paul A. Sandery, Amandine Schaeffer,
18 and Sarath Wijeratne (2016). The Marine Virtual Laboratory (version 2.1):
19 enabling efficient ocean model configuration, *Geosci. Model Dev.*, 9,
20 3297–3307, 2016, <https://doi.org/10.5194/gmd-9-3297-2016>.
21
- 22 Oliveira A, Baptista A (1997) Diagnostic modeling of residence times in
23 estuaries. *Water Resour Res* 33: 1935-1946.
24
- 25 Oliveira, A., J. Rogeiro, G. Jesus, A.B. Fortunato, L. David, M. Rodrigues, J.
26 Costa, T. Mota, J.L. Gomes, R. Matos (2015). Sub-chapter 3.13 - Real-
27 time monitoring and forecast platform to support early warning of faecal
28 contamination in recreational waters. In *Climate Change, Water Supply*
29 *and Sanitation: Risk Assessment, Management, Mitigation and Reduction*,
30 102 - 112. London: IWA Publishing.
31
- 32 Oliveira, A., Fortunato, A.B., Rogeiro, J., Teixeira, J., Azevedo, A. , Lavaud, L.,
33 Bertin, X., Gomes, J., David, M., Pina, J., Rodrigues, M., Lopes, P. (2020).
34 OPENCoastS: An open-access service for the automatic generation of
35 coastal forecast systems, *Environmental Modelling & Software* 124,
36 <https://doi.org/10.1016/j.envsoft.2019.104585>
37
- 38 Orseau, S., Huybrechts, N., Tassi, P., Kaidi, S., Klein, F., 2021. NavTEL: Open-
39 Source Decision Support Tool for Ship Routing and Underkeel Clearance
40 Management in Estuarine Channels, *Journal of Waterway, Port, Coastal,*
41 *and Ocean Engineering*, 147, 2, doi: 10.1061/(ASCE)WW.1943-
42 5460.0000610.
43
- 44 Roberts, K.J., Pringle, W.J., Westerink, J.J., Contreras, M.T., Wirasaet, D.
45 (2019). On the automatic and a priori design of unstructured mesh
46
47
48
49
50
51
52
53
54
55
56
57
58
59
60
61
62
63
64
65

1 resolution for coastal ocean circulation models, *Ocean Modelling*, 144:
2 101509.

3 Rodrigues, M., Fortunato, A.B. (2017). Assessment of a three-dimensional
4 baroclinic circulation model of the Tagus estuary (Portugal). *AIMS*
5 *Environmental Science*, 4(6), 763-787.
6 doi:10.3934/environsci.2017.6.763.

7
8
9
10 Rodrigues, M., Rogeiro, J., David, L., Fortunato, A.B., Oliveira, A. (2016).
11 Análise de sensibilidade à incerteza dos forçamentos na previsão da
12 qualidade da água em tempo real. *Atas do 13º Congresso da Água*
13 (Lisboa, Portugal), 15pp.

14
15
16 Rodrigues, M., Fortunato, A.B., Freire, P. (2019). Saltwater intrusion in the
17 upper Tagus estuary during droughts. *Geosciences*, 9(9), 400. doi:
18 10.3390/geosciences9090400

19
20
21 Roland, A., Zhang, Y. J., Wang, H. V., Meng, Y., Teng, Y.-C., Maderich, V.,
22 Brovchenko, I., Dutour-Sikiric, M., Zanke, U. (2012). A fully coupled 3D
23 wave-current interaction model on unstructured grids, *Journal of*
24 *Geophysical Research*, 117(C11).

25
26
27 Stanev, E.V., Schulz-Stellenfleth, J., Staneva, J., Grayek, S., Grashorn, S.,
28 Behrens, A., Koch, W., and Pein, J. (2016) Ocean forecasting for the
29 German Bight: from regional to coastal scales, *Ocean Science*, 12, 1105-
30 1136

31
32
33 Stokes, K., Poate, T., Masselink, G., King, E., Saulter, A. and Ely, N. (2021)
34 Forecasting coastal overtopping at engineered and naturally defended
35 coastlines, *Coastal Engineering*, 164, 103827,
36 <https://doi.org/10.1016/j.coastaleng.2020.103827>.

37
38
39
40 Trotta, F., Fenu, E., Pinardi, N., Bruciaferri, D., Giacomelli, L., Federico, I.,
41 Coppini, G. (2016) A Structured and Unstructured grid Relocatable ocean
42 platform for Forecasting (SURF), *Deep Sea Research Part II: Topical*
43 *Studies in Oceanography*, Volume 133, Pages 54-75,
44 <https://doi.org/10.1016/j.dsr2.2016.05.004>.

45
46
47
48
49 Trotta F, Federico I, Pinardi N, Coppini G, Causio S, Jansen E, Iovino D and
50 Masina S (2021) A Relocatable Ocean Modeling Platform for
51 Downscaling to Shelf-Coastal Areas to Support Disaster Risk Reduction.
52 *Front. Mar. Sci.* 8, 642815. doi: 10.3389/fmars.2021.642815.

53
54
55
56 Turner, P., Baptista, A.M. (1993). *ACE/gredit User's Manual. Software for*
57 *Semi-automatic Generation of Two-Dimensional Finite Element Grids.*

Center for Coastal and Land-Margin Research, Oregon Graduate Institute of Science & Technology.

- 1
2
3
4
5
6
7
8
9
10
11
12
13
14
15
16
17
18
19
20
21
22
23
24
25
26
27
28
29
30
31
32
33
34
35
36
37
38
39
40
41
42
43
44
45
46
47
48
49
50
51
52
53
54
55
56
57
58
59
60
61
62
63
64
65
- Umgiesser, G., Bajo, M., Ferrarin, C., Cucco, A., Lionello, P., Zanchettin, D., Papa, A., Tosoni, A., Ferla, M., Coraci, E., Morucci, S., Crosato, F., Bonometto, A., Valentini, A., Orlic, M., Haigh, I.D., Nielsen, J.W., Bertin, X., Fortunato, A.B., Gómez, B.P., Fanjul, A.A., Paradis, D., Jourdan, D., Pasquet, A., Mourre, B., Tintoré, J., Nicholls, R.J., in press. The prediction of floods in Venice: methods, models and uncertainty, *Natural Hazards and Earth System Science*. DOI: 10.5194/nhess-2020-361
- Valente AS, Silva JCB (2009). On the observability of the fortnightly cycle of the Tagus estuary turbid plume using MODIS ocean colour images. *Journal of Marine Systems*, 75 (1-2), 131-137.
- Vaz N, Dias JM (2014). Residual currents and transport pathways in the Tagus estuary, Portugal: the role of freshwater discharge and wind, *Journal of Coastal Research*, Special Issue 70, 610-615.
- Viegas, C.N., S. Nunes, R. Fernandes, R. Neves, 2009. Streams contribution on bathing water quality after rainfall events in Costa do Estoril-a tool to implement an alert system for bathing water quality, *Journal of Coastal Research*, Special Issue 56, part 2: 1691-1695
- Wang, Z., Chai, F., Dugdale, R., Liu, Q., Xue, H., Wilkerson, F., Chao, Y., Zhang, Y., and Zhang, H. (2020) The interannual variabilities of chlorophyll and nutrients in San Francisco Bay: A modeling study. *Ocean Dynamics*. 70, 1169-1186. <https://doi.org/10.1007/s10236-020-01386-0>
- The WAVEWATCH III R Development Group (WW3DG) (2016). *User manual and system documentation of WAVEWATCH III R version 5.16*. Tech. Note 329, NOAA/NWS/NCEP/MMAB, College Park, MD, USA, 326 pp.
- Werner, M., J. Schellekens, P. Gijbers, M. van Dijke, O. van den Akker, K. Heynert, (2013). The Delft-FEWS flow forecasting system, *Environmental Modelling & Software*, 40, 65–77.
- Wolf, B., Kiel, E., Hagge, A., Krieg, H.-J., Feld, C.K. (2009). Using the salinity preferences of benthic macroinvertebrates to classify running waters in brackish marshes in Germany. *Ecological Indicators*, 9, 837-847.
- Zhang, Y., Ateljevich, E., Yu, H.-C., Wu, C.-H., Yu, J.C.S. (2015). A new vertical coordinate system for a 3D unstructured-grid model. *Ocean Modelling*, 85, 16-31. <https://doi.org/10.1016/j.ocemod.2014.10.003>

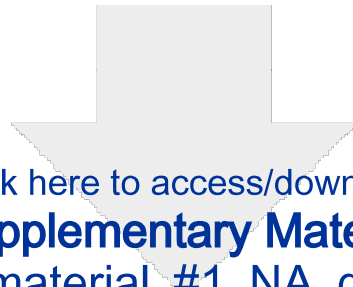
Zhang, Y.J., Ye, F., Stanev, E.V., Grashorn, S., 2016. Seamless cross-scale modeling with schism. *Ocean Modelling*, 102, 64–81.

1
2
3
4
5
6
7
8
9
10
11
12
13
14
15
16
17
18
19
20
21
22
23
24
25
26
27
28
29
30
31
32
33
34
35
36
37
38
39
40
41
42
43
44
45
46
47
48
49
50
51
52
53
54
55
56
57
58
59
60
61
62
63
64
65

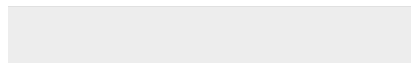
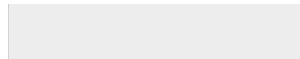
Declaration of interests

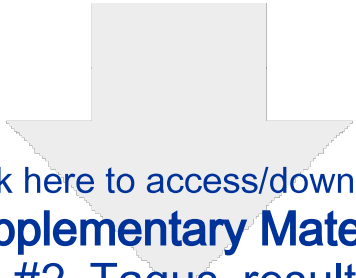
The authors declare that they have no known competing financial interests or personal relationships that could have appeared to influence the work reported in this paper.

The authors declare the following financial interests/personal relationships which may be considered as potential competing interests:



Click here to access/download
Supplementary Material
Suppl_material_#1_NA_grid.docx





[Click here to access/download](#)

Supplementary Material

Suppl_material_#2_Tagus_results_stations.docx

